Article

Discovery of Recent thecideide brachiopods (Order: Thecideida, Family: Thecideidae) in Sulawesi, Indonesian Archipelago, with implications for reproduction and shell size in the genus *Ospreyella*

ERIC SIMON[1] & JANA HOFFMANN[2]

[1]*Department of Palaeontology, Belgian Royal Institute for Natural Sciences, Vautier Street, 29, B-1000 Brussels, Belgium.*
E-mail: ericsimon98brach@yahoo.fr
[2]*Museum für Naturkunde, Leibniz-Institut für Evolutions- und Biodiversitätsforschung, Invalidenstraße 43, D-10115 Berlin, Germany.*
E-mail: jana.hoffmann@mfn-berlin.de

Table of contents

Abstract

For the first time thecideide brachiopods have been discovered in the Indonesian Archipelago. All specimens were collected in a water depth of 30 m from an old shipwreck, the "Mutiara", which represents a remarkable habitat for these cryptic brachiopods despite its artificial nature. The thecidellinine species *Minutella* cf. *minuta* and the lacazelline species *Ospreyella mutiara* **n. sp.** are described and illustrated comprehensively, including their shell ontogeny. The inclusion of the new species *O. mutiara* in the genus *Ospreyella* Lüter and Wörheide, 2003 is based on results of an integrated approach combining morphological, ontogenetic and genetic studies. Relevant morphological characters diagnostic for *Ospreyella* are established. In addition, all Recent lacazelline brachiopod genera are confirmed as valid taxa using molecular methods. The small body size of *O. mutiara* and the weakly developed brachidium in comparison to other *Ospreyella* species as a

consequence of heterochrony is discussed in more detail. *O. mutiara* is the first species of the exclusively gonochoristic genus *Ospreyella* for which hermaphroditism is now documented.

Key words: Brachiopoda, *Minutella*, *Ospreyella*, new species, hermaphroditism, heterochrony, shell ontogeny

Introduction

Thecideide brachiopods are small cementing articulated brachiopods. They live in cryptic habitats and have a world-wide tropical and subtropical distribution. Thecideides have a long fossil record extending back to the Upper Triassic (Baker 2006). Baker (1990) provided a revised taxonomy for this group, evaluating opinions about thecideide classification and ancestry prior to the 1970's in the light of more recent findings. He provided a commonly accepted classification for the Treatise on Invertebrate Paleontology (Baker 2006, 2007). Recent representatives of the Thecideoidea Gray, 1840 are only known from the families Thecidellinidae Elliott, 1958 and Thecideidae Gray, 1840. The subfamily Thecidellininae Elliott, 1958 belonging to the family Thecidellinidae comprises two Recent genera, *Thecidellina* Thomson, 1915 and *Minutella* Hoffmann and Lüter, 2010. The subfamily Lacazellinae belonging to the family Thecideidae Gray, 1840 comprises three Recent genera, *Pajaudina* Logan, 1988, *Lacazella* Munier-Chalmas, 1880 and *Ospreyella* Lüter and Wörheide, 2003. The position of the genus *Kakanuiella* Lee and Robinson, 2003 currently assigned to the family Thecidellinidae is debated by Lee and Robinson (2003), Lüter (2005) and Baker (2007).

At the beginning of the 20th century only a few Recent thecideide brachiopod species were known. In recent years continuous research including trawling or dredging and, in particular, investigations of cryptic environments by SCUBA diving increased the discovery of new genera (Logan 1988; Hoffmann & Lüter 2010) and several new species (Logan 2005; Lüter 2005; Logan 2008; Lüter *et al.* 2008; Hoffmann & Lüter 2009; Hoffmann *et al.* 2009; Hoffmann & Lüter 2010).

In the Indo-Pacific region several species of the thecidellinine genus *Thecidellina* are known, such as *Thecidellina japonica* (Hayasaka, 1938), *Thecidellina congregata* Cooper, 1954, *Thecidellina maxilla* (Hedley, 1899), *Thecidellina insolita* Hoffmann, Klann and Matz, 2009, and *Thecidellina blochmanni* Dall, 1920. In 1981, Cooper described *Thecidellina minuta,* a minute brachiopod trawled from the Samper Bank, southeast of Madagascar, Indian Ocean. A revision of this material allowed Hoffmann and Lüter (2010) to include this species in the new genus *Minutella* together with two new Caribbean species: *M. tristani* Hoffmann and Lüter, 2010 (type species) and *M. bruntoni* Hoffmann and Lüter, 2010. A number of specimens from localities all over the West-Pacific Ocean, e.g. Japan, Fiji, and Great Barrier Reef, have been assigned by these authors to the species *Minutella minuta* based on strong morphological similarity. Furthermore, they described a morphological separation of Caribbean/ Atlantic and Indo-Pacific representatives of *Minutella* by the shape of the median septum. Bitner (2010) documented *Thecidellina minuta*, now assigned to *Minutella* cf. *minuta* (pers. com. J. Hoffmann), also from New Caledonia.

Representatives of the lacazellines genus *Ospreyella* Lüter and Wörheide, 2003 are known from different regions in the Pacific and Indian Ocean. The type species of this genus, *Ospreyella depressa* Lüter, 2003, was collected from submarine caves at Osprey Reef, Queensland, Australia. Logan (2005) described *O. maldiviana* from submarine caves at Addu Atoll and South Male Atoll in the Maldives Islands which was the first documentation of representatives of the genus *Ospreyella* in the Indian Ocean. In 2008, Logan described *Ospreyella palauensis* from Chandelier cave, Koror Island, Palau. In addition, specimens collected from Lizard Island, Great Barrier Reef, possibly juvenile forms, were described as *Ospreyella* sp. by Hoffmann *et al.* (2009).

"*Lacazella*" *mauritiana* Dall, 1920 is the only species of the exclusively Atlantic genus *Lacazella* described from the Indian Ocean (Mauritius). Cooper (1973) provided the first illustration of the type specimen. *Lacazella mauritiana* was also mentioned by Zezina (1985, 1987) who found this species among material collected by the BENTHEDI-Cruise in the Mozambique Channel. Unfortunately, the type material of *L. mauritiana* is lost (Logan 2005) and thus a proper species description cannot be provided to date. In the Pacific Ocean *Lacazella* sp. is documented from submarine caves in Okinawa, Japan (Motchurova-Dekova *et al.* 2002; Saito *et al.* 2002), and shallow waters around New Caledonia (Bitner 2010). There is ongoing discussion on the affiliation of *Lacazella mauritiana* to the genus *Ospreyella* and not *Lacazella* (pers. com. J. Hoffmann). The assignation of lacazelline specimens in the Indian and Pacific Ocean to the genus *Lacazella* will be discussed later in this paper.

SIMON & HOFFMANN

In the last two decades investigation of ontogenetic patterns has become more and more important for taxonomic studies of Recent thecideide brachiopods. Lee and Robinson (2003) already proposed that ontogenetic and molecular studies should be associated with morphological observations. In 2004, Logan provided a first comprehensive description of the shell development in the lacazelline brachiopod *Pajaudina atlantica* Logan, 1988. In 2008, Logan compared the shell ontogeny of the lacazelline species *Ospreyella palauensis* from Palau with the thecidellinine species *Thecidellina congregata* from Saipan. A complete series of ontogenetic stages of the Caribbean thecidellinine species *Thecidelina meyeri* has been provided by Hoffmann and Lüter (2009). Hoffmann and Lüter (2010) then compared the overall shell development of the thecidellinine genera *Thecidellina* and *Minutella* and of different species of the genus *Thecidellina* from the Atlantic and Pacific Ocean. Furthermore, Baker and Logan (2011) illustrated additional developmental series of *Thecidellina* sp. from Europa Island in the Indian Ocean and *Minutella bruntoni* from the Cayman Islands in the Caribbean as examples of Recent representatives in their work on common pattern in the early shell development in Recent and fossil representatives of Thecideoidea.

In this study the presence of thecideide brachiopods in the Indonesian Archipelago is documented for the first time, which extends their geographical range in the Indo-Pacific region. The material investigated was collected in proximity of the harbour of Donggala in the Bay of Palu (Province of Central Sulawesi) on the western coast of Sulawesi (Strait of Makassar) inside a shipwreck. The submerged holds of the wreck are extremely dark places and acts as almost closed submarine caves. These ecological conditions are very favourable for the establishment of cryptic brachiopod populations (Simon 2010) as a permanent water current inside the shipwreck provides continuously a food supply. The metal walls of the holds are covered with an abundant epifauna dominated by brachiopod specimens. Thecideides were the most abundant brachiopods among these. However, megathyrid brachiopods such as *Joania arguta* (Grant, 1983) and *Argyrotheca furtiva* Simon, 2010, the terebratellid brachiopod *Frenulina sanguinolenta* (Gmelin, 1792), a rhynchonellid species and a *Novocrania* species were also part of this community documented by Simon (2010).

In the investigated material two thecideide species were found and assigned to the thecidellinine genus *Minutella* Hoffmann and Lüter 2010 and the lacazelline genus *Ospreyella* Lüter and Wörheide, 2003. Their taxonomic assignation and position is discussed in more detail based on morphological, ontogenetic and, for the first time, molecular investigations. The detailed documentation of the shell development allows a direct comparison with other already documented Recent thecideide brachiopods. Furthermore, additional data on adult shell size, sex ratios, and sex related morphological characters are provided. Their relevance for the understanding of reproduction modes in Recent thecideides is discussed in more detail.

Material and methods

All brachiopod specimens investigated in this study were collected in August 2009 by SCUBA diving in an old shipwreck in the harbour of Donggala, Central Sulawesi, Indonesia (Text-Fig. 1). The shipwreck, the "Mutiara", sank 58 years ago at the entrance to the harbour and is now at a depth of 30 m. The top layer of the muddy sediment was collected from the seafloor in the shipwreck and subsequently washed and sieved. A sieve of 0.5 mm was used for extraction of the smallest fractions. The sieved material was air dried and the individual brachiopod shells were hand-picked under a stereo microscope. The study of numerous dead brachiopod specimens, which were accumulated post-mortem in the sediment, provided important information on mortality and was useful for the understanding of the reproduction mode based on sexual dimorphic shell characters. Specimens possessing a marsupial notch are considered as functional females and those lacking a marsupial notch as males, respectively.

Several fragments of the metal walls of the "Mutiara" were collected with specimens kept in living position and with preserved soft tissue. Half of the fragments removed from the walls of the wreck were air dried. The remaining fragments were preserved in 70% ethanol.

Shells of specimens selected for scanning electron microscopy (SEM) were treated with household bleach (5% hypochlorite) in order to remove all remaining soft body parts. Specimens collected alive were preserved in ethanol and passed through successive ethanol/formaldehyde dimethyl-acetal treatments (respectively 100/0 – 75/25 – 25/75 – 0/100 in %) and were subsequently critical-point dried. All the samples for SEM were mounted, sputter coated with gold, and investigated using a low vacuum SEM (ESEM FEI Quanta 200).
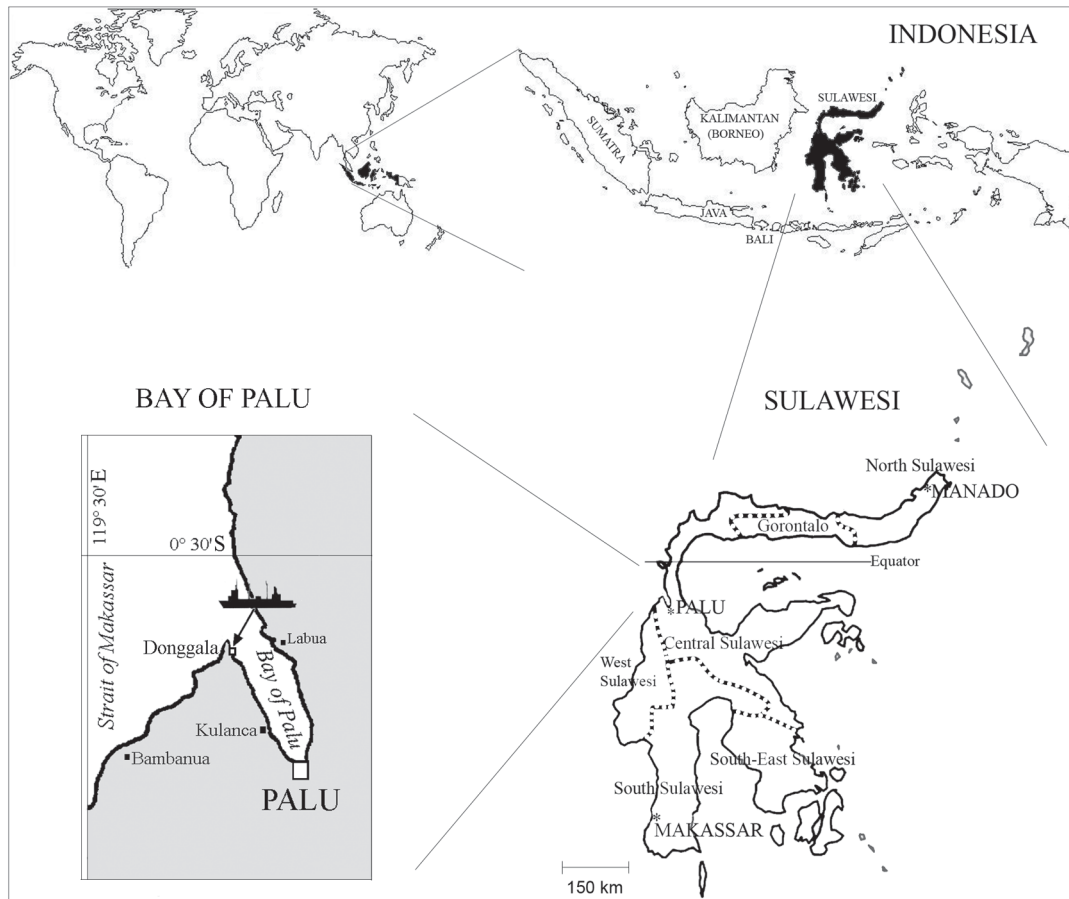
TEXT-FIGURE 1. Map of Indonesia and local maps of Sulawesi showing the collecting site, the shipwreck "Mutiara" (water depth: 30 m), which sank off the harbour of Donggala (Bay of Palu, Strait of Makassar, Sulawesi Central, Indonesia).

Several specimens preserved in ethanol (100%) were used for molecular studies. Individual specimens were kept separated and the soft tissue for DNA extraction, e.g. gonads and parts of the lophophore, was analysed individually and not pooled. Genomic DNA extractions were performed using a standard CTAB protocol (Winnepenninckx *et al.* 1993). The small subunit of the nuclear ribosomal RNA gene (18S rDNA), was amplified using the primers F 19 5´- ACC TGG TTG ATC CTG CCA-3´ with R 1843 5´- GGA TCC AAG CTT GAT CCT TCT GCA GGT TCA CCT AC-3´ resulting in one fragment of c. 1526 bp or by amplification of three overlapping fragments using either primer combinations F 19 5´- ACC TGG TTG ATC CTG CCA-3´ with R 993 5´- CTT GGC AAA TGC TTT CGC-3´, F 439 5´- GTT CGA TTC CGG AGA GGG A-3´ with R 1372 5´- GAG TCT CGT TCG TTA TCG GA-3´, F 1012 5´- GCG AAA GCA TTT GCC AAG MA-3´ with R 1843 5´- GGA TCC AAG CTT GAT CCT TCT GCA GGT TCA CCT AC-3´ (pers. com. B. Cohen). PCR conditions included an initial 94 °C denaturation of 90 s, followed by 35 cycles of 30 s at 94 °C, 2.3 min ranging from 55-58 °C, followed by a final 10 min extension 72 °C extension. Amplification of the three overlapping 18S rDNA fragments included an initial 94 °C denaturation of 90 s, followed by 35 cycles of 30 s at 94 °C, 2 min at 55 °C, followed by a final 5 min 72 °C extension. PCR products were sequenced in both directions. BigDye v.3.1 Terminator (Applied Biosystems, Foster City, California) was used for the sequencing reaction, and sequences were produced on an Applied Biosystems 3130xl Genetic Analyser at the Humboldt University of Berlin. Sequence chromatograms were visually edited against chromatograms of complementary strands using BioEdit version 7.0.9.0 (Hall 1999) and FinchTV version 1.4.0 (Geospiza, available at www.geospiza.com).

The 18S rDNA data set comprises 16 sequences representing 12 in-group representatives (lacazellines) and 4 out-group representatives (thecidellinines). The sequences were aligned in MEGA5 (Tamura *et al.* 2011) using CLUSTAL W, v. 1.81 (Thompson *et al.* 1994) with gap opening or extension penalties 15/4 (default parameters) and local realignment of highly variable regions. Ambiguously aligned sites were removed using Gblocks 0.91b (Castresana 2000) using default parameters.

SIMON & HOFFMANN

Phylogenetic relationships were inferred by Maximum parsimony, Maximum likelihood and Neighbor-Joining in Paup*4b10. Maximum likelihood analyses were performed with the evolutionary model GTR+I+G selected by AICc in Modeltest 3.7.

Specimens illustrated in this paper have been deposited under general IG 31 862 in the collections of the Department of Recent Invertebrates of the Belgian Royal Institute for Natural Sciences in Brussels (RBINS). Specimens sent to the Museum für Naturkunde Berlin, Germany, for comparative morphological studies are deposited under ZMB Bra 2264-2265. Each molecular sample investigated is represented by a voucher specimen (shell) and deposited at the Museum für Naturkunde Berlin, Germany. The obtained DNA samples were either used up or are stored at -80°C at the Museum für Naturkunde in Berlin, Germany. GenBank accession numbers for each sequence are provided (Table 1).

Suprafamilial classification follows Williams *et al.* (1996) and the hierarchy within the superfamily Thecideoidea Gray, 1840 follows Baker (2006, p. H1948-1964). The terminology for morphological descriptions of the thecidellinine genus *Minutella* follows Hoffmann and Lüter, 2009 (p. 470, fig. 2, p. 472), and for the lacazelline genus *Ospreyella* follows Hoffmann *et al.* 2009.

Results

Taxonomy

PHYLUM BRACHIOPODA DUMÉRIL, 1806
SUBPHYLUM RHYNCHONELLIFORMEA WILLIAMS *ET AL.*, 1996
CLASS RHYNCHONELLATA WILLIAMS *ET AL.*, 1996
ORDER THECIDEIDA ELLIOTT, 1958
SUPERFAMILY THECIDEOIDEA GRAY, 1840
FAMILY THECIDELLINIDAE ELLIOTT, 1958
SUBFAMILY THECIDELLININAE ELLIOTT, 1953

Genus *Minutella* Hoffmann and Lüter, 2010

Diagnosis. See Hoffmann and Lüter (2010), p. 142.
Type species. *Minutella tristani* Hoffmann and Lüter, 2010.

***Minutella* cf. *minuta* (Indonesia)**
Pl. 1, Figs 1–5; Pl. 2, Figs 1–8

Material investigated. The material was collected from the shipwreck "Mutiara", water depth: 30 m, Bay of Palu, off Donggala Harbour, Donggala near Palu, Province of Central Sulawesi, Indonesia. 131 complete shells, 19 dorsal valves and 11 ventral valves were obtained from the sieved sediment. 53 complete adult specimens, nine complete juvenile specimens and 11 ventral valves were obtained from air dried samples of fragments of the metal wall of the shipwreck. Six complete adult specimens and three complete articulate juvenile specimens were obtained from fragments of the metal wall preserved in ethanol. The material investigated in this study is deposited in the collections of the Belgian Royal Institute for Natural Sciences (RBINS) and some samples are deposited in the Museum für Naturkunde Berlin.

TABLE 1. Material used for molecular analyses (18S rDNA) with additional information, such as species name, voucher number, locality, collector and accession number.

| No.[1]	Genus	Species name	Locality (water depth)	Collector	GenBank Accession No.
Ospreyella					
56 (D1414)	Ospreyella	depressa	Osprey Reef, Great Barrier Reef, Australia	G. Wörheide	KC577455
57[2]	Ospreyella	cf. palauensis	Okinawa, Japan	don. B. Cohen 2007	KC577456
128	Ospreyella	mutiara n.sp	ship wreck "Mutiara", Donggala, Propinsi Sulawesi Tengah, Indonesia, (30 m)	N. Ulakaba	KC577452
129	Ospreyella	mutiara n.sp	ship wreck "Mutiara", Donggala, Propinsi Sulawesi Tengah, Indonesia, (30 m)	N. Ulakaba	KC577451
130	Ospreyella	mutiara n.sp	ship wreck "Mutiara", Donggala, Propinsi Sulawesi Tengah, Indonesia, (30 m)	N. Ulakaba	KC577453
131	Ospreyella	mutiara n.sp	ship wreck "Mutiara", Donggala, Propinsi Sulawesi Tengah, Indonesia, (30 m)	N. Ulakaba	KC577454
Pajaudina					
3	Pajaudina	atlantica	Puerto Naos, La Palma, Canary Islands (20 m)	G. Maghon	KC577457
16	Pajaudina	atlantica	Puerto Naos, La Palma, Canary Islands (20 m)	G. Maghon	KC577457
Lacazella					
6	Lacazella	caribbeanensis	Disco Bay, Jamaica (10-15 m)	G. Jaecks	KC577459
89	Lacazella	caribbeanensis	Turneffe Island (St. 23), Belize, Caribbean (13 m)	ALDEBARAN Exp., J. Hoffmann & C.O. Coleman	KC577460
90	Lacazella	caribbeanensis	Turneffe Island (St. 23), Belize, Caribbean (13 m)	ALDEBARAN Exp., J. Hoffmann & C.O. Coleman	KC577461
93	Lacazella	caribbeanensis	San Pedro (St. 24), Belize, Caribbean (23 m)	ALDEBARAN Exp., J. Hoffmann & C.O. Coleman	KC577462
outgroup					
21	Thecidellina	sp.	Banc Arago, DW1968, French Polynesia (120-100 m)	BENTHAUS Cruise, R.B. de Forges	KC577463
49	Thecidellina	williamsi	Sal, Cape Verde (15 m)	P. Wirtz	KC577464
76	Thecidellina	japonica	near Kurose, off Hachijo-jima Island (100-200 m)	JAMSTEC, H. Namikawa	KC577465
91	Minutella	sp.	Turneffe Island (St. 23), Belize, Caribbean (13 m)	ALDEBARAN Exp., J. Hoffmann & C.O. Coleman	KC577466

[1] Internal voucher numbers.
[2] There is no voucher of this material deposited as the donation only included the DNA sample.

Description. Fully grown adult shells are rather small (Table 2), rarely reaching more than 2 mm, longer than wide; strongly ventribiconvex (Pl. 1, Fig. 1d–e). The relationships between ratios length/width (L/W) and width, length of dorsal valve/width (LDV/W) and width, thickness/width (T/W) and width, and length of hinge line/width (WH/W) and width are illustrated in Text-Fig. 2. The shell is endopunctate, with large punctae. The anterior commissure is rectimarginate (Pl. 1, Fig. 1e). The lateral commissure is straight. The hinge line is straight and its length represents 50 to 75% of the maximum width of the shell (Table 2).

TABLE 2. *Minutella* cf. *minuta* (Cooper, 1981). Morphometric measurements were taken from 48 specimens. Ratios were calculated for each individual and are not based on the maximum and minimum values of the entire sample. All measured shells are dead adult specimens extracted from the sieved sediments collected from the holds of the shipwreck. L: length (mm); W: width (mm); T: thickness (mm); LDV: length of dorsal valve (mm); WH: width of the hinge line (mm). L/W= ratio length to width, T/W= ratio thickness to width, LDV/W= ratio length of dorsal valve to width, WH/W= ratio width of hinge line to width.

n = 48	L [mm]	W [mm]	T [mm]	LDV [mm]	WH	L/W	T/W	LDV/W	WH/W
MIN	1.40	1.21	0.47	0.87	0.60	1.07	0.35	0.67	0.47
MAX	2.14	1.67	1.27	1.44	1.07	1.37	0.82	1.06	0.74
MEAN	1.74	1.43	0.91	1.20	0.87	1.22	0.64	0.84	0.61
Standard error	± 0.02	± 0.02	± 0.03	± 0.02	± 0.02	± 0.01	± 0.02	± 0.01	± 0.01
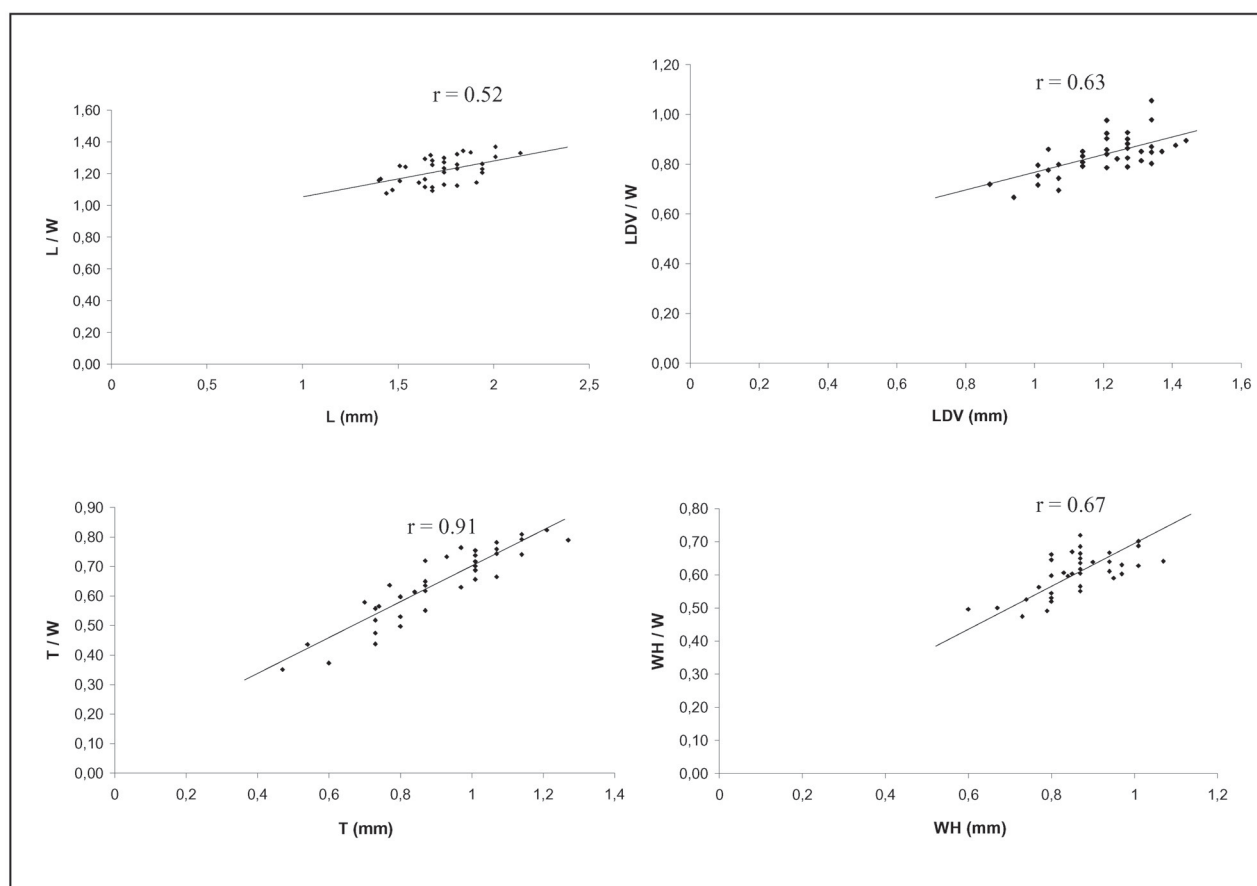
TEXT-FIGURE 2. Scatterplots of morphometric measurements of *Minutella* cf. *minuta* (Cooper, 1981) specimens. L: length (mm); W: width (mm); LDV: length of dorsal valve (mm); T: thickness (mm); WH: length of hinge line (mm). Relationships between ratios L/W and width, LDV/W and width, T/W and width, and WH/W and width. Linear regression and correlation coefficient (r) indicated.
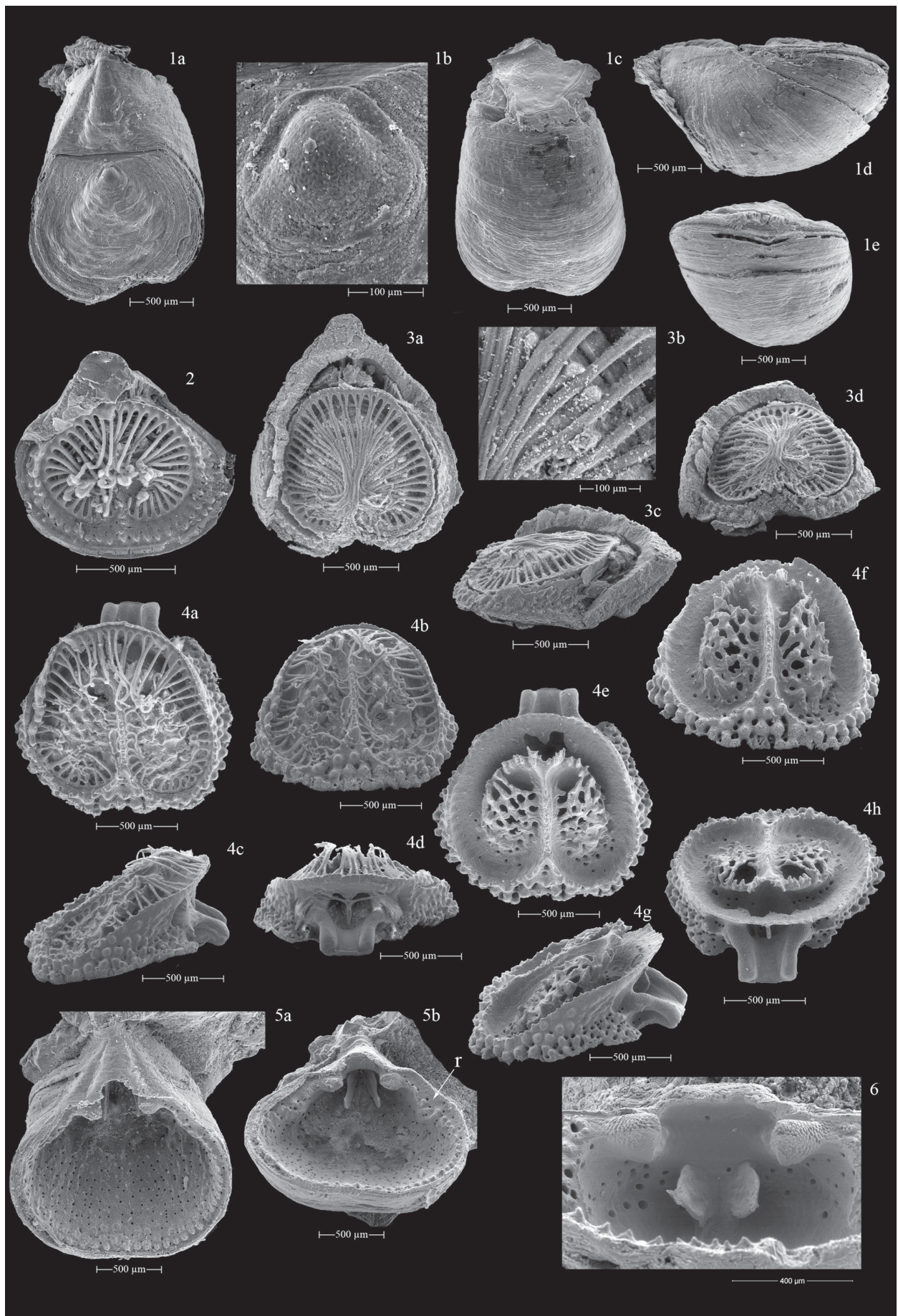
The ventral valve is elongate, often cemented by its posterior part but sometimes additionally by its ventral surface. The interarea is transversely striated and flanks a long, slender and dorsally convex pseudodeltidium (Pl. 1, Figs 1a, 5a). The teeth are short, robust and covered with secondary shell material. Their surface is finely corrugated (Pl. 1, Fig. 6). A very narrow smooth groove, the peripheral groove (after Zumwalt 1976, p. 29; "g" in Pl. 1, Fig. 5b), runs along the internal side of the commissure. On the internal side of this groove a row of strong tubercles is developed. The valve floor is granulose or smooth, densely punctate, appears roughly striated (Pl. 1, Fig. 5a), but is not tuberculated. The hemispondylium (Pl. 1, Figs 5b, 6) comprises two long, thin prongs which are subparallel to slightly diverging anteriorly and fused with the posterior part of the ventral valve floor. No septum was observed in the ventral valve floor.

The dorsal valve is smaller than the ventral valve, transversely ovate, often gently rounded anteriorly but sometimes emarginated. Numerous growth lines are visible on the external valve surface. The valve is slightly convex and the protegulum is placed at the tip of the valve (Pl. 1, Figs 1c–d). The surface of the protegulum is wrinkled (Pl. 1, Fig. 1b). Internally, the dorsal valve has a progressively raised profile towards its posterior part (Pl. 1, Fig. 4g; Pl. 2, Fig. 1d, 1e). The outer margin is strongly tuberculated but an external very narrow smooth flange is observed (this part of the shell is easily broken and often it is only partly visible; "fl" in Pl. 2, Fig. 1d). A straight, thin, very narrow median septum is developed. Anteriorly the septum has short divergent margins. The ventral side of this septum is ornamented with small spines and a short groove is visible anteriorly but it does not extend toward the median and posterior part (Pl. 1, Fig. 4e; Pl. 2, Fig. 1a). The peribrachial ridge is heavily tuberculated. The brachial cavities are covered with canopying spicules protecting the brood pouches. The brachial cover built by the canopying spicules is rather stout, made of subovate holes having a variable diameter and a subconical structure (Pl. 2, Fig. 1b). The marsupial holes are large with irregular spiny margins. The brachial bridge is broad and its ventral side is finely denticulated (Pl. 2, Fig. 1h). The interbrachial ridge is very spiny and irregular (Pl. 1, Fig. 4h; Pl. 2, Fig. 1f). The visceral gap is relatively large and it is divided by a very slender, lamellar calcitic pole. The pole

PLATE 1. *Minutella* cf. *minuta*. Size of the specimens indicated with scale bars.

Fig. 1. RBINS- RI-BRA 9. A complete articulated adult shell still attached in living position to a shell fragment. This specimen has been collected from the sieved sediment found in the ship wreck 1a: Dorsal view. 1b: Prominent protegulum with wrinkled surface. 1c: Ventral view illustrating the attachment of specimens by the ventro-posterior part of the ventral valve. 1d: Lateral view showing the irregular growth lines. 1e: Anterior view showing the ventribiconvex aspect of the shell.

Fig. 2. RBINS-RI-BRA 10. A juvenile specimen collected alive and preserved in ethanol. Dorsal valve with preserved lophophore. At this stage of growth the lophophore is schizolophe with 40 relatively thick tentacles. The median septum is emerging anteriorly.

Fig. 3. RBINS-RI-BRA 11. Specimen at a later stage of growth, collected alive and preserved in ethanol. Dorsal valve with preserved lophophore. The lophophore is schizolophe with 60 tentacles. The median septum is more developed and canopying spicules are covering the brachial cavities. 3a: Ventral view. A small fragment of the ventral valve remained attached to the dorsal valve. 3b: Detail of the lophophore tentacles that are spaced by the top of the canopying spicules.

Fig. 4. RBINS-RI-BRA 12. An adult specimen collected alive and preserved in ethanol. Dorsal valve with preserved lophophore. The lophophore with up to 75 relatively thin tentacles covers the brood pouches which are protected by the canopying spicules. The narrow straight median septum is clearly defined. **4a**: Ventral view. **4b**: Oblique anterior view. A narrow groove is developed on the ventral side of the median septum. **4c**: Lateral view. Strongly tuberculated outer margin and cardinal process. **4d**: Posterior view. The visceral foramen is divided by the slender calcitic pole which is not fused with the base of the cardinal process. Lateral adductor muscles are visible on either side of the visceral foramen and diductor muscle scars on the posterior margin of the cardinal process. **4e**: The same dorsal valve in ventral view, bleached for removing all organic parts. Canopying spicules are forming subovate holes (marsupial holes). **4f**: Oblique anterior view. The intrabrachial ridges are spiny and the crest of the median septum is very narrow. **4g**: Lateral view. The spiny intrabrachial ridges and posterior outgrowth of the calcitic pole are visible. **4h**: Oblique posterior view. The marsupial holes and the posterior outgrowth of the calcitic pole are well-defined. One median adductor muscle scar in the visceral cavity is visible.

Fig. 5. RBINS-RI-BRA 13. A ventral valve of an adult specimen. **5a**: Dorsal view with interarea, pseudodeltidium, teeth and roughly striated ventral valve floor. **5b**: Anterior view with the hemispondylium consisting of two long prongs.

Fig. 6. RBINS-RI-BRA 14. A smaller adult ventral valve of a specimen still attached in living position to the substrate. Detailed oblique anterior view with anterior part of the pseudodeltidium and hemispondylium. The teeth are corrugated.
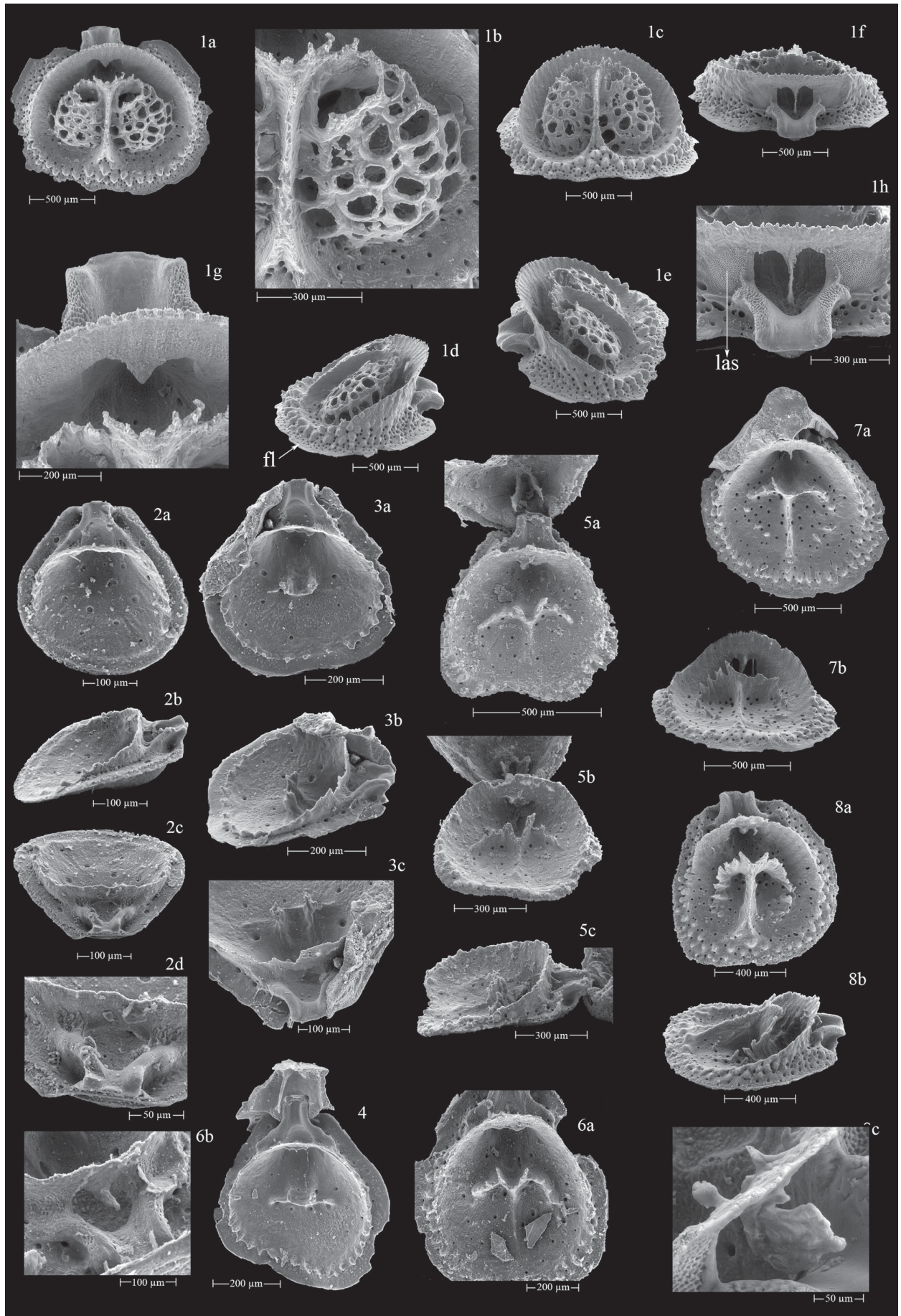
is attached to the brachial bridge by a short conical structure which appears as a triangle from the anterior (Pl. 1, Fig. 4e; Pl. 2, Fig. 1g). The calcitic pole is never fused with the ventral surface of the cardinal process and is protruding posteriorly as a flabelliform plate which is sometimes quite broad and irregular (Pl. 2; Fig. 1e, 8c). The cardinal process is short, strong and subquadrate with thick lateral lobes. The median lobe is anteriorly subdued. Lateral adductor muscle scars, placed on either side of the visceral gap, are subovate or fan-shaped and clearly visible ("las" in Pl. 2, Fig. 1h). The schizolophous lophophore is made of 60–70 tentacles in adult specimens (Pl. 1; Figs 3a, 4a). The imprints of the lophophore groove and lophophore muscles scars are faint and arranged along the inner side of the peribrachial ridge.

Remarks. The *Minutella* specimens from Indonesia are morphologically very similar to *Minutella minuta s.s.* from Samper Bank, Madagascar, as described by Cooper, 1981, and thus assigned to *Minutella* cf. *minuta*. However, they differ in some small morphological details. The median septum has a very similar structure in both species as it is narrow and has spiny ventral margins. In *M. minuta s.s.* the median septum is slightly wider and a groove is reaching to the middle of its length. In *M.* cf. *minuta* the groove is not present. The canopying spicules in *M. minuta s.s.* are slender and the holes formed by these spicules vary in shape. In *M.* cf. *minut*a the holes formed by the canopying spicules are more regular, subovate and relatively large. The calcitic pole of *M. minuta s.s.* is lamellar and develops lateral outgrowths. In *M.* cf. *minuta* the calcitic pole is more slender and develops posterior outgrowths.

◀

PLATE 2. *Minutella* cf. *minuta.* Size of the specimens indicated with scale bars.
Fig. 1. RBINS-RI-BRA 14. A small adult dorsal valve with intact canopying spicules. **1a**: Ventral view. **1b**: Detail of the canopying spicules forming subovate holes with subconical margins. **1c**: Oblique anterior view. **1d**: Oblique lateral view. A very narrow smooth flange (fl) is visible at the commissure. **1e**: Oblique lateral view showing the very thin median septum and the posterior outgrowth of the calcitic pole. **1f**: Posterior view. The calcitic pole is very slender and the ventral side of the intrabrachial ridges is ornamented with strong spines. **1g**: Detail of the cardinal process and the brachial bridge. The median triangular elevation of the calcitic pole is well-defined. **1h**: Posterior view with fan-shaped lateral adductor muscle scars and diductor muscle scars on the posterior margin of the cardinal process.
Fig. 2. RBINS-RI-BRA 15. Earliest juvenile stage of growth observed in the material collected. The brachial bridge starts to develop. The bilobed cardinal process is small and does not extend far beyond the posterior margin of the valve. The peribrachial ridge is defined by tubercles on the lateral margins. Anteriorly the peribrachial ridge is a smooth ridge. The visceral foramen is undivided. The valve floor is smooth. **2a**: Ventral view. **2b**: Oblique lateral view. **2c**: Oblique posterior view.
Fig. 3. RBINS-RI-BRA 16. Juvenile stage with two fused subparallel spikes developing in the middle of the valve floor. The body wall is formed between the two spikes and is expanding laterally (visible on the left part, the right part is broken). The cardinal process is bilobed. The peribrachial ridge is defined by a row of pointed tubercles. The median septum and calcitic pole are absent. **3a**: Ventral view. Small fragments of the ventral valve remained attached to the posterior part of the dorsal valve. **3b**: Oblique lateral view. **3c**: Detailed view of the posterior part of the shell. The brachial bridge is slightly damaged on the left side.
Fig. 4. RBINS-RI-BRA 17. Growth stage with a trilobed cardinal process. In the median part of the brachial bridge the calcitic pole is formed by an outgrowth pointing downwards. The intrabrachial ridges are extending laterally forming the body wall. The peribrachial ridge becomes more prominent.
Fig. 5. RBINS-RI-BRA 18. Specimen with complete dorsal valve and posterior parts of the ventral valve including the hemispondylium. In the dorsal valve the two central fused spikes are growing backwards forming a V-shaped structure. The intrabrachial ridges are reinforced. The median septum appears in the middle of the valve floor. **5a**: Ventral view. **5b**: Oblique anterior view. **5c**: Oblique lateral view. The slender calcitic pole is well developed and its posterior outgrowth is visible.
Fig. 6. RBINS-RI-BRA 19. Slightly more advanced stage of growth. The peribrachial ridge is now defined by two rows of strong tubercles. **6a**: Ventral view. **6b**: Detailed view of the calcitic pole with its posteriorly directed spur.
Fig. 7. RBINS-RI-BRA 10. Growth stage with the median septum reaching the anterior part of the valve and connecting to the peribrachial ridge. Several brachial cavity tubercles are secreted in order to draw the margins of the brachial lobes. **7a**: Ventral view. A fragment of the posterior part of the ventral valve remained attached to the dorsal valve. **7b**: Oblique anterior view. On of the intrabrachial ridge is broken.
Fig. 8. RBINS-RI-BRA 20. In this dorsal valve the construction of the brachial lobes is progressing. The median septum is now diverging anteriorly and fused to the peribrachial ridge forming a triangular structure. **8a**: Ventral view. **8b**: Oblique lateral view. **8c**: Detailed view of the posterior region with calcitic pole. Additional outgrowths are produced by the anterior part of the brachial bridge.

However, all these characters are slightly variable in the material investigated from Donggala. Such a variation has already been pointed out by Hoffmann and Lüter (2010, pp. 150–152) between *Minutella* cf. *minuta*, material collected from Okinawa (Japan), *Minutella* cf. *minuta*, collected from Astrolabe Reef, Dravuni, Fiji, Pacific Ocean, and *Minutella* cf. *minuta*, collected from Lizard Island, Australia. This indicates that small morphological variations do not simply allow the erection of distinct species in the genus *Minutella* originating from the Indo-Pacific region. However, the investigated material from Indonesia supports the observation that all Indo-Pacific forms of the genus *Minutella* share one common character, the blade-like median septum, in contrast to their Caribbean relatives, which exhibit an anteriorly diverging median septum (see also Hoffmann and Lüter 2010).

Family Thecideidae Gray, 1840

Subfamily Lacazellinae Backhaus, 1959

Genus *Ospreyella* Lüter and Wörheide, 2003

Emended diagnosis. Fibrous secondary shell layer vestigial in both valves. Ventral valve interarea pseudodeltidium present; prongs plate-like, medially fused; myophragma present; supporting septum absent. Dorsal valve lophophore ptycholophous; minor interbrachial lobes with further furcations; median ramus delicate structure, attached by narrow bases to valve floor; median crest usually absent; brachial bridge slender, marsupial notch present in females; intrabrachial ridges arch-like, leaving characteristic holes; cardinal process with additional median lobe present, anteriorly subdued; calcitic pole absent. Brooding in one median brood pouch located in ventral valve; specialised tentacles for attachment of larvae present.
    Type species. *Ospreyella depressa* Lüter, 2003

Ospreyella mutiara **n. sp.**
Pl. 3, Figs 1–8; Pl. 4, Figs 1–10; Pl. 5, Figs 1–6; Pl. 6, Figs 1–8; Pl. 7, Figs 1–6

Diagnosis. Small- to medium-sized thecideide brachiopod (maximum size = 4.0 mm, Table 3). Female shells larger than male shells and with a more complete ontogenetic development. Shell whitish, ventribiconvex, slightly uniplicate anteriorly. Ventral valve with short, triangular, convex pseudodeltidium, anterior part with numerous irregular cavities. Sulcus present in most specimens. Ventral valve floor median ridge absent. Hemispondylium formed by two pointed lateral prongs and a prominent median myophragma; supporting structure of hemispondylium absent in adults. Dorsal valve with narrow and straight median ramus with subparallel frilled margins; ramuli relatively narrow, slightly curved, with spiny margins; ventral side of ramus and ramuli weakly convex. Anterior median depression reduced, narrow, anterior margin tuberculated. Minor interbrachial lobes often asymmetrical, straight, short, subparallel, never furcated. Major interbrachial lobes relatively thin with dentate outer margins. Lophophore ptycholophous.
    Etymology. The name is directly derived from the word "*mutiara*". In Indonesian language "*mutiara*" means "pearl". This is the name of the shipwreck where the new species was discovered.
    Type material. Holotype: RBINS-RI-BRA 24 (Plate 3, Figures 4a and 4b), fully grown mature female specimen with marsupial notch, specialised tentacles and median brood pouch with larvae. Paratypes: RBINS-RI-BRA 21-22, 25, 27, 33, 39, 42, 49, 52, 54. The type material is deposited in the Belgian Royal Institute for Natural Sciences (RBINS).
    Type locality. Shipwreck "Mutiara", water depth: 30 m, Bay of Palu, off Donggala Harbour, Donggala near Palu, Province of Central Sulawesi, Indonesia.
    Additional material. Sediment samples from shipwreck, 78 entire shells, 53 dorsal valves and 47 ventral valves; samples picked from metal wall of shipwreck, air-dried, 242 adult specimens, 215 juvenile specimens and 69 ventral valves; specimens picked from metal wall of shipwreck, preserved in ethanol, 115 entire adult shells and 92 entire juvenile shells; ZMB Bra 2264-2265, pieces of metal wall with specimens of *M.* cf. *minuta* and *O. mutiara* **n. sp.**

TABLE 3. *Ospreyella mutiara* **n. sp.** Morphometric measurements were taken from 44 specimens extracted from the sieved sediments exhibiting a marsupial notch and 14 specimens with male features collected alive in the wreck lacking a marsupial notch. L: length (mm); W: width (mm); T: thickness (mm); LDV: length of dorsal valve (mm); WH: width of the hinge line (mm). L/W= ratio length to width, T/W= ratio thickness to width, LDV/W= ratio length of dorsal valve to width, WH/W= ratio width of hinge line to width. n.m.: value not measured.

"Female" specimens[1]	L[mm]	W[mm]	T[mm]	LDV[mm]	WH	L/W	T/W	LDV/W	WH/W
Holotype RBINS - RI -BRA 24	2.4	2.8	1.6	1.8	1.34	0.86	0.57	0.64	0.48
Paratype RBINS - RI - BRA 39	2.6	3.0	n.m.	2.4	2.09	0.87	n.m.	0.81	0.70
Paratype RBINS - RI - BRA 27	3.1	3.0	1.9	2.1	1.7	1.04	0.65	0.71	0.58
Paratype RBINS - RI - BRA 25	2.6	2.7	n.m.	1.8	1.4	0.95	n.m.	0.66	0.53
Paratype RBINS - RI -BRA 54	3.2	3.2	n.m.	2.3	2.2	0.98	n.m.	0.70	0.68
Paratype RBINS - RI - BRA 21	3.0	3.0	1.9	2.2	1.9	1.01	0.63	0.72	0.63
Paratype RBINS - RI - BRA 22	2.4	2.8	1.6	1.9	1.4	0.87	0.58	0.68	0.50
N ♀ (Total)	44	44	41	44	44	44	41	44	44
N (collected alive)	13	13	10	13	13	13	10	13	13
N (dead shells in sediment)	31	31	31	31	31	31	31	31	31
MIN	2.4	2.7	1.3	1.8	1.3	0.83	0.40	0.58	0.44
MAX	4.0	3.9	2.4	2.6	2.7	1.18	0.80	0.81	0.83
MEAN	3.2	3.2	1.9	2.2	2.0	1.02	0.59	0.69	0.63
Standard error	±0.06	±0.04	±0.05	±0.03	±0.05	±0.02	±0.02	±0.01	±0.01
"Male" specimens[2]	L[mm]	W[mm]	T[mm]	LDV [mm]	WH	L/W	T/W	LDV/W	WH/W
Paratype RBINS - RI - BRA 33	2.3	2.7	n.m.	1.8	1.5	0.87	n.m.	0.68	0.54
Paratype RBINS - RI - BRA 52	1.9	2.2	n.m.	1.6	1.0	0.85	n.m.	0.71	0.45
Paratype RBINS - RI - BRA 49	1.7	2.0	n.m.	1.4	1.0	0.86	n.m.	0.71	0.48
Paratype RBINS - RI - BRA 42	n.m.	2.1	n.m.	1.6	0.9	n.m.	n.m.	0.79	0.43
N ♂ (Total)	14	16	9	16	16	14	9	16	16
N (collected alive)	11	13	6	13	13	11	6	13	13
N (dead shells on *Neopycnodonte*)	3	3	3	3	3	3	3	3	3
MIN	1.7	2.0	0.5	1.4	0.7	0.81	0.18	0.60	0.35
MAX	2.7	3.0	1.7	2.2	2.0	1.00	0.64	0.90	0.70
MEAN	2.3	2.4	1.0	1.7	1.3	0.9	0.36	0.73	0.52
Standard error	±0.09	±0.14	±0.15	±0.10	±0.05	±0.02	±0.06	±0.02	±0.03

[1] specimens with marsupial notch; [2] specimens lacking marsupial notch.

Description. External shell characters: The endopunctate shell is relatively small for the genus (Table 3), reaching a width of about 3 mm, variable in shape (Table 3). The maximum width (W) is at the mid-dorsal valve (Pl. 3, Fig. 1a). The value of the length to width (L/W) ratio increases during growth and the shells become slightly longer than wide (Text-Fig. 3). The whitish shell has an irregularly elongate shape and is cemented to the substrate by the posterior and ventral part of the ventral valve. Due to this type of attachment, the posterior part of the shell is often truncate and can be distorted. The shell is strongly ventribiconvex (Pl. 3, Fig. 1b), the dorsal valve being relatively flat, lid-like, except for its median part which is slightly convex. During growth the thickness of the shell increases relatively to its width, as indicated by the changing thickness to width (T/W) ratio (Text-Fig. 3). A
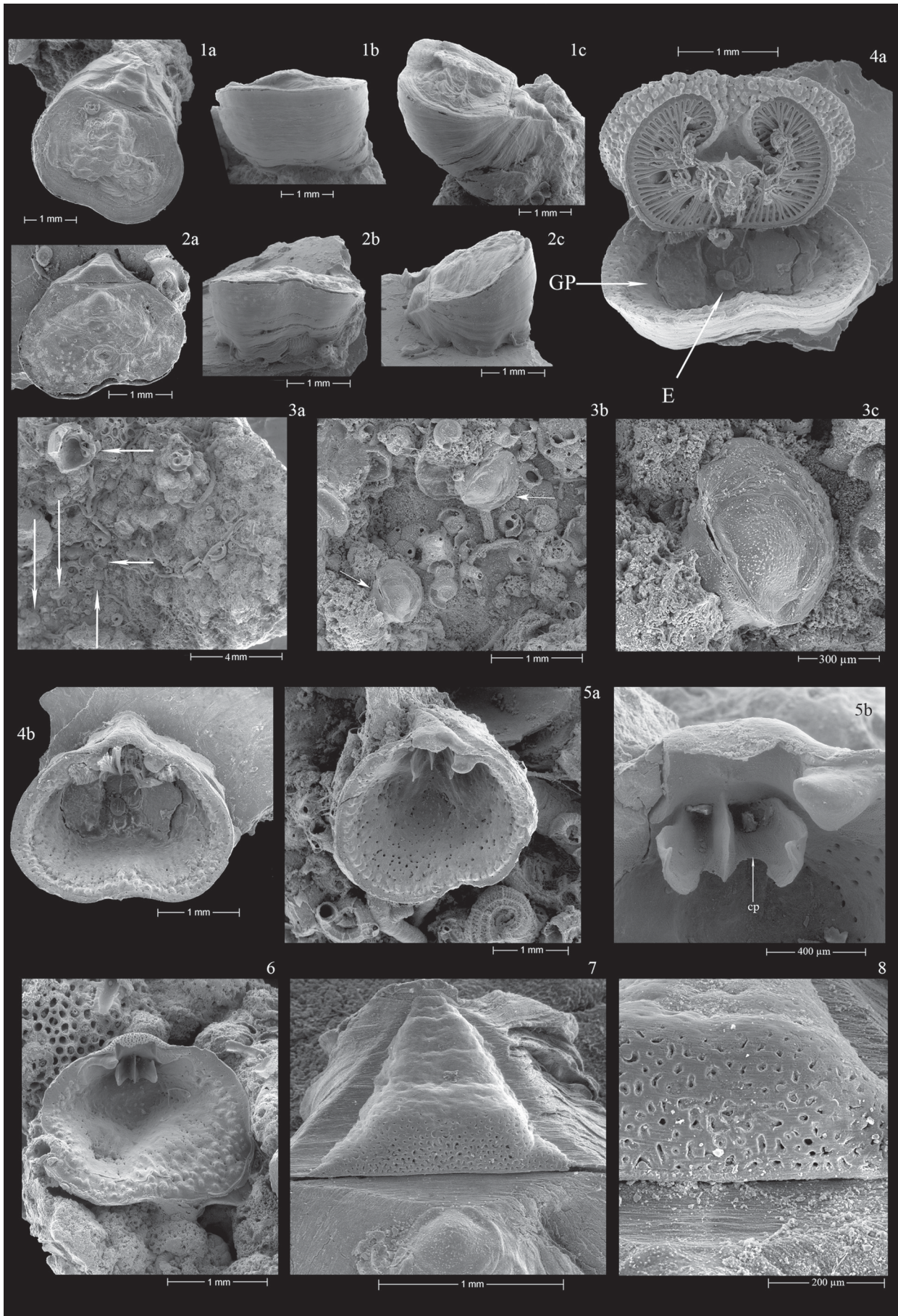
median low sulcus can develop at the anterior margin of the ventral valve (Pl. 3, Fig. 2b) resulting in a slight cordiform shape of the dorsal valve. The entire shell is lifted from the substrate anteriorly (Pl. 3, Fig. 1c), its anterior part tending to be in a more elevated position than its posterior part. Such a geniculation of the ventral valve is common in thecideide brachiopods as already illustrated by Pajaud (1970; p. 219, fig. 130A). The anterior commissure is variable, rectimarginate to slightly uniplicate or sometimes slightly unisulcate. The lateral commissure is gently concave dorsally.

The ventral valve has a short but strongly produced beak with a flat triangular interarea ornamented with numerous fine regular growth lines parallel to the hinge line. A raised triangular, transversely convex pseudodeltidium is developed (Pl. 3, Fig. 7). The pseudodeltidium is relatively long, representing till 25 % of total shell length and has irregular growth lines on its surface (Pl. 3, Fig. 7). The anterior part of the pseudodeltidium is perforated by numerous irregular cavities which do not represent punctae (Pl. 3, Fig. 7–8). Irregular growth lines are visible on the external ventral shell surface (Pl. 3, Fig. 1b).
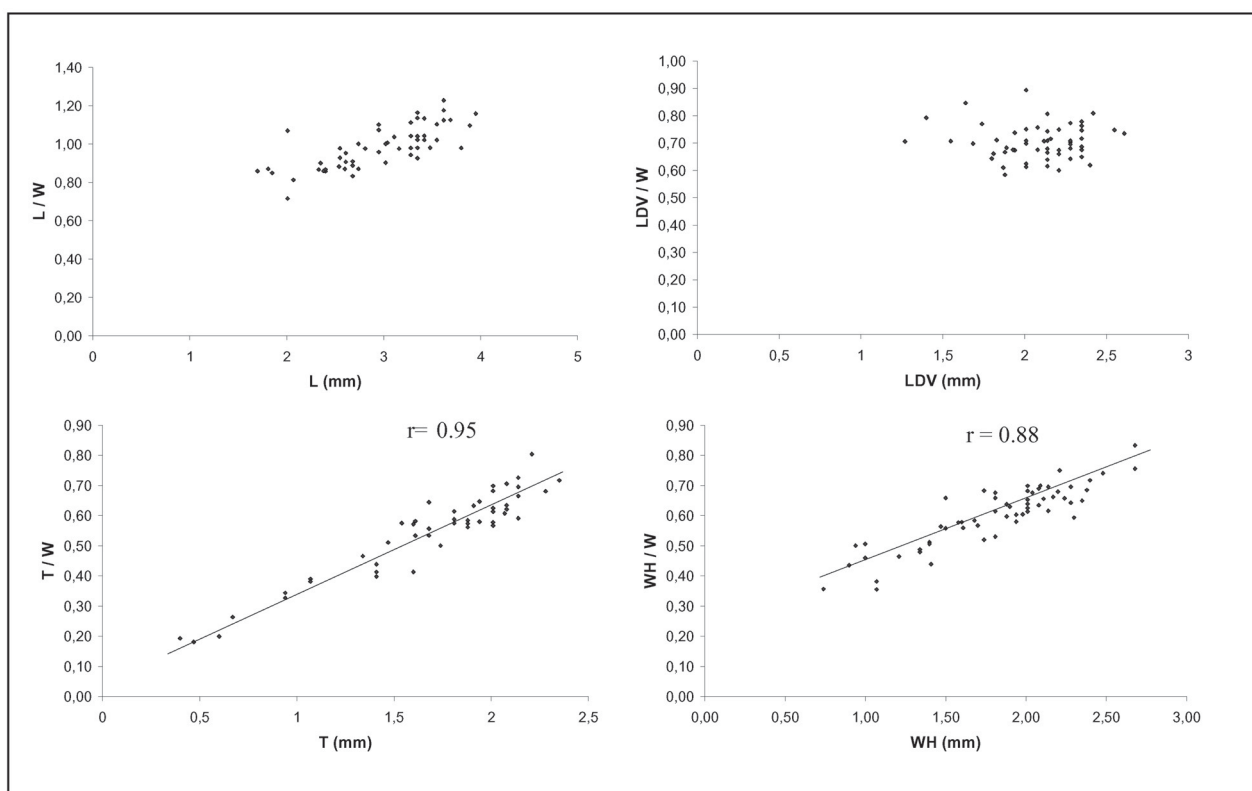
TEXT-FIGURE 3. Scatterplots of morphometric measurements of *Ospreyella mutiara* **n. sp.** specimens. L: length (mm); W: width (mm); LDV: length of dorsal valve (mm); T: thickness (mm); WH: length of hinge line (mm). Relationships between ratios L/W and width; LDV/W and width; T/W and width; WH/W and width. Linear regression applied when significant and correlation coefficient (r) indicated.

The lid-like dorsal valve is always wider than long, subrectangular (Pl. 5, Fig. 1a) to transversely ovate (Pl. 5, Fig. 5a) in shape with an emarginated anterior commissure. The dorsal valve in larger specimens is subrectangular (Pl. 5; Figs 1a, 2a, 3a), whereas the dorsal valve in smaller specimens is more transversely ovate (Pl. 5; Figs 5a, 6a). This variability in shape is related to the size of the specimen as the value of the length of the dorsal valve to width (LDV/W) ratio (Text-Fig. 3) does not change throughout growth. The dorsal valve surface exhibits irregular growth lines. The surface of the prominent protegulum (if preserved) is wrinkled. The hinge line is straight and always narrower than the maximum width of the valve (Table 3). Its length represents 55 % (mean value) of the maximum width of the shell. However, the length of hinge line can increase up to 83% of the width of the shell (Table 3). In fact, in comparison with the maximum width of the shell, the length of the hinge line increases during growth as indicated by the values of the width of the hinge to the width of the shell (WH/W) ratio (Text-Fig. 3).

Figure labels: 1a, 1b, 1c, 2a, 2b, 2c, 4a, GP, E, 3a, 3b, 3c, 4b, 5a, 5b, cp, 6, 7, 8

Scale bars: 1 mm, 1 mm, 1 mm, 1 mm, 1 mm, 1 mm, 1 mm, 4 mm, 1 mm, 300 μm, 1 mm, 1 mm, 400 μm, 1 mm, 1 mm, 200 μm

Internal shell characters: The cordiform or slightly bilobed ventral valve has a roughly striated surface valve floor without a median ridge and exhibits large and irregular endopunctae (Pl. 3, Fig. 5a). The commissure is limited internally by a row of more or less regular, strong tubercles, and externally a smooth rim is developed. The cyrtomatodont strong teeth are short and relatively thick and covered with secondary shell material. Their surface is corrugated. The hemispondylium consists of two pointed lateral prongs and a prominent median myophragma (Pl. 3, Fig. 5b). A supporting septum of the hemispondylium cannot be observed in adult or young specimens. However, in juveniles a temporary very small supporting structure is developed in a few cases ("s.s." in Pl. 6, Fig. 7b). No median ridge is present in the ventral valve. Two calcitic oval pads covering the gonads are clearly visible in the posterior part of the ventral valve floor ("GP" in Pl. 3, Fig. 4a). In large ("female") specimens a median brood pouch containing several larvae ("L" = larvae in Pl. 3, Fig. 4a) is situated between these gonad pads.

In the dorsal valve the subperipheral rim is heavily papillose, with strong irregular tubercles. These tubercles are generally ornamented with striated secondary shell fibres on their tips (Pl. 5, Fig. 7). A very narrow smooth flange is present along the commissure. The dental sockets are strong and formed by a thick, curved inner socket ridge and a flat depressed outer socket ridge (Pl.5, Fig.1c). The trilobed cardinal process (Pl. 5, Fig. 3c) is wide, massive but relatively short and slightly curved dorsally. The development of the median lobe is variable as it appears sometimes very prominent (Pl. 5, Fig. 1h) or sometimes rather weak (Pl. 5, Fig. 3g). Shell structures developed in the dorsal valve are raised towards the posterior part of the valve (Pl. 5, Figs 1c, 2c, 3f, 5c). A thin and relatively narrow brachial bridge (Pl. 5, Fig. 1h) is built by the fusion of the posterior parts of the inner rim margin (similar to a fusion of crural processes as proposed by Logan 2008, p. 411). This brachial bridge remains complete in small specimens (Pl. 5, Figs. 5e, 6d) but is interrupted in larger specimens by a prominent marsupial notch (Pl. 5, Figs 1h, 2d, 3h). The marsupial notch is a small circular hole open on its ventral side. The posterior face of the marsupial notch exhibits a small platform with a small convex median ridge prolonged by a small pointed spur (Pl. 5, Figs 1h, 4a, 4b). The inner surface of the marsupial notch exhibits the muscle scars of the specialized filaments. Between the cardinal process and the brachial bridge a heart-shaped visceral foramen (Pl. 5, Fig. 1h), free of a calcitic pole, is apparent. On each side of the visceral foramen, on the posterior part of the inner rim margin, the

PLATE 3. *Ospreyella mutiara* **n. sp.** Size of the specimens indicated with scale bars.
Fig. 1. RBINS-RI-BRA 21, paratype. This fully grown adult is still attached to the substrate. **1a**: Dorsal view. **1b**: Anterior view showing the ventribiconvex shell. **1c**: Oblique lateral view. The shell is curved upwards and is more elevated in its anterior part. Irregular growth lines are visible.
Fig. 2. RBINS-RI-BRA 22, paratype. Young specimen attached to the substrate (shell of *Neopycnodonte*). At this stage of growth the shell is mainly attached by the posterior ventral side of the ventral valve. **2a**: Dorsal view. The pseudodeltidium and the prominent protegulum with its wrinkled surface are clearly visible. **2b**: Anterior view. A weak sulcus in the anterior part of the ventral valve is visible. **2c**: Oblique lateral view.
Fig. 3. RBINS-RI-BRA 23. A piece of metallic substrate from the store in the shipwreck with several juvenile specimens of *O. mutiara* **n. sp.** (arrows) **3a**: Overview. **3b**: Detailed view of two juvenile specimens attached to the substrate. At this stage of growth, the posterior part of the ventral valve is very prominent. **3c**: Detailed view of one juvenile specimen. The pseudodeltidium exhibits irregular cavities at its anterior margin. The surface of the protegulum is wrinkled.
Fig. 4. RBINS-RI-BRA 24, holotype. The specimen is an adult specimen with a median brood pouch and larvae (L). Critical point dried. **4a**: Opened complete articulated specimen showing the lophophore in living position. Specialized tentacles are located at the posterior part of the lophophore. **4b**: Dorsal view of ventral valve showing detached fibres of the adductor and diductor muscles in the posterior part of the specimen. Two calcitic oval pads cover the gonads in the visceral cavity. Exposed larvae are visible between the calcitic pads in the posterior part of the valve.
Fig. 5. RBINS-RI-BRA 25, paratype. Adult ventral valve attached to the substrate. The two calcitic oval pads covering the gonads are missing. **5a**: Dorsal view showing the peripheral ridge, the surface of the valve floor, the interarea, the pseudodeltidium and one tooth. The left tooth is broken. **5b**: Detailed view of the hemispondylium which consists of two pointed lateral lobes and a prominent median myophragm.
Fig. 6. RBINS – RI – BRA 26, paratype. Juvenile ventral valve attached to the substrate. The sculptured surface of the anterior part of the pseudodeltidium is very apparent. The ventral valve is coalesced with the substrate.
Fig. 7. RBINS-RI-BRA 27, paratype. Dorsal view of the posterior part of the ventral valve. The interarea exhibits fine sub-parallel growth lines. The pseudodeltidium is convex. The hinge line is straight. The prominent protegulum exhibits a wrinkled surface.
Fig. 8. RBINS-RI-BRA 22, paratype. Dorsal view of the pseudodeltidium and the hinge line of the ventral valve.
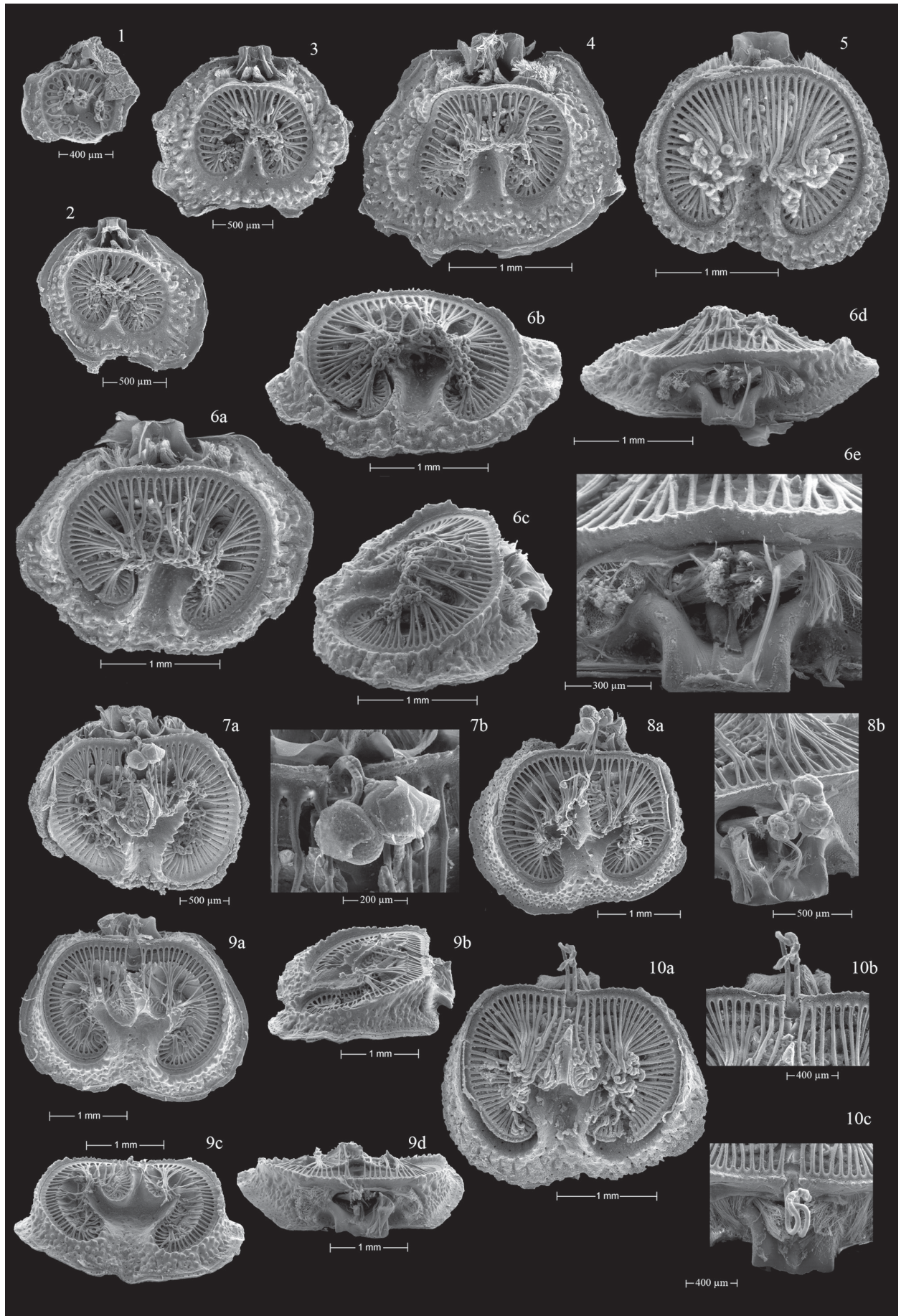
reniform lateral adductor muscle scars are clearly visible (Pl. 5, Figs 1d, 2d, 3g, 5d, 5c). The diductor muscle scars are sometimes visible on the posterior margin of the cardinal process (Pl. 5, Figs 1h, 5d) but they are often poorly defined. The median adductor muscle scars are present in the visceral cavity on either side of the visceral foramen (Pl. 5, Fig. 1f). The margins of the intrabrachial ridges exhibit short strong spines. Underneath the intrabrachial ridges a pair of residual small holes (Pl. 5, Fig. 1a) is present which is filled by shell material in most adults during growth (Pl. 5, Fig. 2a). The outer margins of the major interbrachial lobes are connected to the jugum (Pl. 5, Fig. 1g) and exhibit dentate margins. The two subparallel minor interbrachial lobes are relatively short, thick and never divided or furcated in any specimens observed. The development of the minor interbrachial lobes is often asymmetrical (Pl. 5, Figs 2a, 3a). The pointed median ramus has a slightly concave upper surface, subparallel and frilled lateral margins and is connected posteriorly by the small jugum (Pl. 5, Fig. 1g) to the intrabrachial ridges. The length of the median ramus is variable and terminates in the middle of the valve or sometimes at about two-thirds of the valve length. The median ramus is attached to the valve floor by a triangular base developed in the anterior part of the valve (Pl. 6, Figs 5b, 6b, 6c). Two strong lateral ramuli are well-developed. Each ramulus is relatively narrow but as wide as the median ramus and their upper surface is slightly concave. The lateral margins of the ramuli are ornamented with four to six strong spines on both sides. The concavity of the upper surface of the ramuli tends to decrease with progressive growth. In most adult stage the concavity observed is rather weak as shell material fills this cavity progressively during growth (Pl. 5, Fig. 3c). A narrow median anterior depression is developed, its anterior margin being invaded by strong tubercles. Sometimes, this median depression is absent (Pl. 5, Fig. 2a). This is especially observed when the growth of the anterior part of the valve is disrupted (Pl. 5, Fig. 3a).The ascending apparatus and the descending apparatus can be developed symmetrically (Pl. 5, Fig. 1a) but frequently a strong dissymmetrical development of the dorsal valve structures is observed (Pl. 5, Fig. 2a). The adult

PLATE 4. *Ospreyella mutiara* **n. sp.** Size of the specimens indicated with scale bars.
Fig. 1. RBINS-RI-BRA 28, paratype. Very early juvenile stage with a trocholophe lophophore possessing 27 tentacles. Lateral adductor and median adductor muscles visible on the left side of the shell.
Fig. 2. RBINS-RI-BRA 29, paratype. Early juvenile stage with a schizolophe lophophore possessing 48 tentacles. The median ramus precursor is developed.
Fig. 3. RBINS-RI-BRA 30, paratype. Juvenile with schizolophe lophophore consisting of 55 tentacles. The median ramus is widening. Detached lateral adductor and median adductor muscle fibres are visible.
Fig. 4. RBINS-RI-BRA 31, paratype. Developmental stage with ptycholophe lophophore. Detached lateral adductor and median adductor muscle fibres are visible.
Fig. 5. RBINS-RI-BRA 32, paratype. Specimen considered as "male" with further developed median ramus and ramuli. A marsupial notch is missing.
Fig. 6. RBINS-RI-BRA 33, paratype. One of the largest specimens with male features. No marsupial notch is apparent. **6a**: Ventral view. **6b**: Oblique anterior view pointing out the narrow median anterior depression. **6c**: Oblique lateral view. **6d**: Posterior view. The brachial bridge exhibits no marsupial notch. **6e:** Detailed view of the entire median portion of the brachial bridge.
Fig. 7. RBINS-RI-BRA 34, paratype. One of the smallest specimens with female features. This specimen considered as "female" possesses a brooding apparatus. Two larvae are attached to the specialized tentacles, which are removed from the median brood pouch in the ventral valve. **7a**: Ventral view. The median ramus and the ramuli are further developed than in the largest shell with male features. **7b**: Detailed view of the larvae attached to the specialized tentacles. Fragments of the broken brood pouch are still covering the larvae.
Fig. 8. RBINS-RI-BRA 35, paratype. Specimen with female features. Three larvae are attached to the specialized tentacles. The median ramus and the ramuli are well developed. **8a**: Ventral view. **8b**: Detailed view of the marsupial notch with specialized tentacles and attached larvae.
Fig. 9. RBINS-RI-BRA 36, paratype. A larger specimen with female features. Marsupial notch and specialized tentacles are present. No larvae are attached to the tip of the tentacles. The tentacles of the lophophore are perfectly spaced by spines on top of the major interbrachial lobe. **9a**: Ventral view. Noteworthy is the strong ventral concavity of the ramuli at this stage of growth. **9b**: Oblique lateral view. The narrow smooth flange running along the outer margin of the valve is perfectly preserved in this sample. **9c**: Oblique anterior view with lifted median ramus and ramuli. The anterior median depression is inconspicuous. **9d**: Posterior view.
Fig. 10. RBINS-RI-BRA 37, paratype. Fully grown specimen with female features. The median ramus is uplifted and exhibits a very narrow concave crest. The anterior median depression is inconspicuous. **10a**: Ventral view. **10b**: Detailed anterior view of the marsupial notch with specialized tentacles. **10c**: Detailed posterior view of the marsupial notch with specialized tentacles.
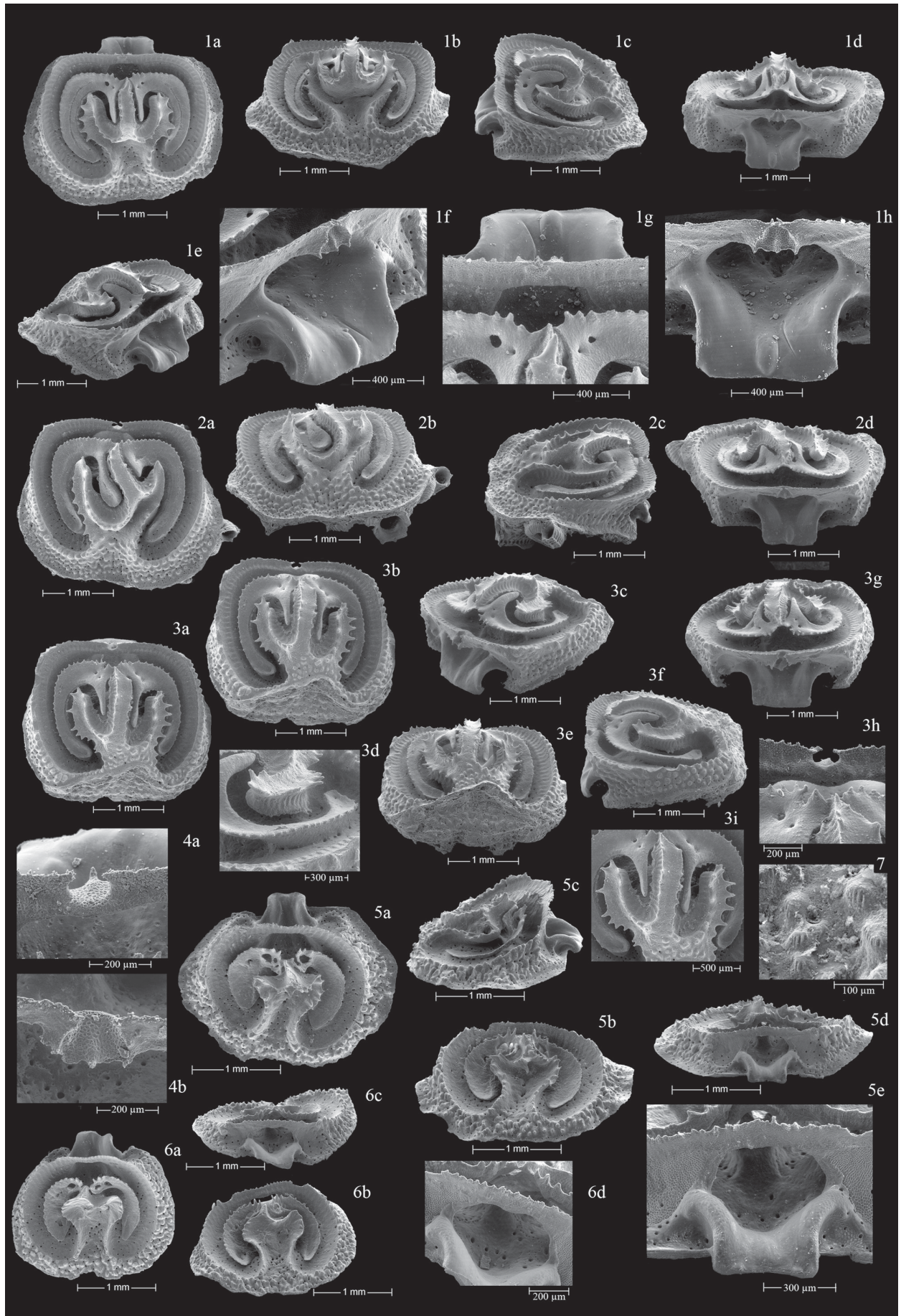
lophophore is ptycholophous with 140/150 tentacles observed in an adult female specimen (Pl. 4, Fig. 9a). Male specimens are smaller and their lophophore consists of a lower number (± 50) of tentacles (Pl. 4, Fig. 6a). The lophophore is attached to the lophophore groove which follows the internal side of the peribrachial ridge, the external sides of the ramuli and the lateral sides of the median ramus (Pl. 5, Figs 3b, 3d). Lophophore muscle scars are parallel and clearly defined. At the trocholophe stage, the lophophore possesses 27 tentacles (Pl. 4, Fig. 1) but this number increases rapidly and 46 tentacles are observed in a young schizolophe developmental stage (Pl. 4, Fig. 2). In smaller adult specimens, the lophophore is developed regularly (Pl. 4, Fig. 6a). In larger adult specimen (females), the lophophore is interrupted posteriorly, allowing the development of a pair of specialized median tentacles (Pl. 4, Figs 7a, 8a, 9a, 10a).

Remarks. A comparison of morphological characters which vary between accepted *Ospreyella* species is given in Table 4. A detailed comparison of *O. mutiara* with unidentified *Ospreyella* species from Lizard Island and New Caledonia is given below.

PLATE 5. *Ospreyella mutiara* **n. sp.** Size of the specimens indicated with scale bar.
Specimens with female features:
Fig. 1. RBINS-RI-BRA 38, paratype. A subrectangular valve with two symmetrical minor interbrachial lobes of equal length. **1a**: Ventral view. **1b**: Oblique anterior view. The two ramuli are still relatively incised and they exhibit spiny margins. The median depression is reduced and quite shallow. **1c**: Oblique lateral view. The minor interbrachial lobes are rather wide. Parallel lophophore muscle scars are clearly visible. **1d**: Posterior view. The brachial bridge is narrow and exhibits a marsupial notch. The cardinal process is trilobed. The reniform lateral adductor muscle scars are well defined. **1e**: Oblique latero-posterior view. **1f**: Detailed oblique latero-posterior view showing the brachial bridge with marsupial notch, the cardinal process and the sockets. **1g**: Detailed oblique antero-posterior view illustrating the anterior structure of the marsupial notch, the jugum and anterior structure of intrabrachial ridges. **1h**: Detailed posterior view of the cardinal process and the brachial bridge with marsupial notch. The marsupial notch is a small platform with a small convex median bridge prolonged by a small pointed spur. The inner surface of the marsupial notch exhibits muscle scars of the tentacles muscle fibres.
Fig. 2. RBINS – RI – BRA 39, paratype. A subrectangular valve with strongly asymmetrical structure and with a development of two very unequal minor interbrachial lobes. The median ramus grew obliquely because the unusual development of the right ramulus was more rapid in this ontogenetic process. The median depression is nearly absent in this specimen. **2a**: Ventral view. **2b**: Oblique anterior view. **2c**: Oblique lateral view. **2d**: Oblique posterior view.
Fig. 3. RBINS-RI-BRA 40, paratype. A subrectangular valve with slightly asymmetrical minor interbrachial lobes. The anterior part of the valve is modified which is supposedly caused by environmental influence. The growth has been impaired by a barrier on the substrate. The median depression is inconspicuous. The narrow smooth commissural flange is now located near the anterior part of the median ramus. The space between this flange and the median ramus is heavily tuberculated. **3a**: Ventral view. **3b**: Oblique anterior view. **3c**: Oblique latero-posterior. **3d**: Detailed view of a minor interbrachial lobe and associated ramulus. **3e**: Oblique anterior view showing the modification of the anterior part of the shell. **3f**: Oblique lateral view. **3g**: Oblique posterior view. **3h**: Detailed oblique anterior view of the marsupial notch and of jugum. **3i**: A detailed ventral view of the median ramus and ramuli.
Fig. 4. RBINS.-RI-BRA 41, paratype. A detailed illustration of the marsupial notch. **4a**: Oblique antero-posterior view. The brachial bridge is interrupted medially by an incomplete notch which is opened ventrally. A longitudinal median ridge is perceptible on the platform of the marsupial notch and a relatively long spur is visible. **4b**: Oblique posterior view of the same marsupial notch with the specialized tentacles muscle scars.
Specimens with male features:
Fig. 5 – RBINS-RI-BRA 33, paratype. One of the largest specimens found in the material with a transversely ovate dorsal valve. The ontogenetic development has just produced a small median ramus and very short ramuli. The residual holes in the intrabrachial ridges are still large. The brachial bridge is complete without marsupial notch. **5a**: Ventral view. **5b**: Oblique anterior view. The large spines on the intrabrachial ridges are clearly visible. **5c**: Oblique lateral view. **5d**: Oblique posterior view. **5e**: Detailed oblique posterior view of the visceral gap with complete brachial bridge.
Fig. 6 – RBINS-RI-BRA 42, paratypes. A smaller specimen with a transversely ovate dorsal valve and strong asymmetrical shell structure (only one ramulus has been produced here). The ontogenetic development is still less advanced in this specimen. The jugum and the complete brachial bridge are clearly visible. **6a**: Ventral view. **6b**: Oblique anterior view. **6c**: Oblique posterior view showing complete brachial bridge.
Details of shell structure:
Fig. 7 – RBINS-RI-BRA 36, paratype. Tubercles covering the outer shell margin. The tip of the tubercles is ornamented with vertical ridges formed by secondary shell fibres. The number of ridges is relatively variable (the specimen illustrated here is also visible on Pl. 4, Fig. 9).
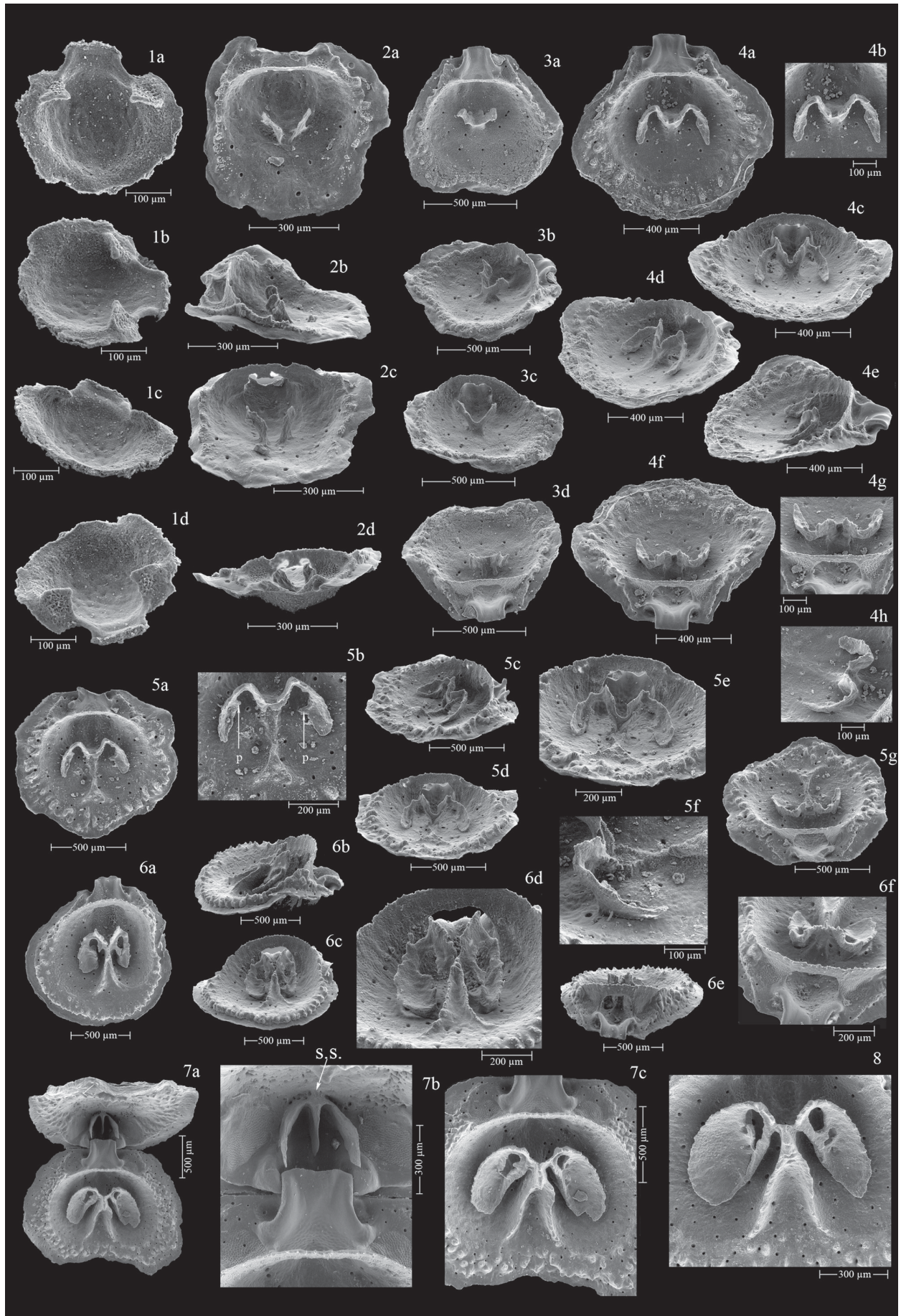
The *Ospreyella* specimen from Lizard Island (Australia) has many juvenile aspects (Hoffmann *et al.* 2009). However, these specimens seem to be adult as the shell illustrated a mature specimen with a marsupial notch (width: 1.75 mm; Hoffmann *et al.* 2009, Fig. 4j). In this specific case, this mature specimen (female) did not develop any minor interbrachial lobes. It seems to have shortened its shell development and its morphological structures are even more ephebic than in *O. mutiara* **n. sp.**

The material of "*Lacazella*" sp. from New Caledonia dredged at a water depth of 105–110 m (Bitner 2010, Fig. 6) is a collection of dead shells and resembles *O. mutiara* **n. sp.** to a large degree. The shape and the size of the shells are very similar. The minor interbrachial lobes are straight, without furcations, and asymmetrical. However, some differences with *O. mutiara* **n. sp.** are perceptible. The median depression in "*Lacazella*" sp. is wider and smooth. The ramuli are further developed, wider, strongly incised and their margins are not dentate. In *O. mutiara* **n. sp.** the ramuli are quite narrow, not deeply incised and their margins are strongly frilled. It is assumed that "*Lacazella*" sp. is actually a representative of the genus *Ospreyella* (pers. comm. J. Hoffmann).

PLATE 6. Ontogenetic stages of *Ospreyella mutiara* **n. sp.** Size of the specimens indicated with scale bars.

Fig. 1. RBINS-RI-BRA 43, paratype. The earliest stage of growth found in this study. The cardinal process is bilobed and very short. Lateral adductor muscle scars already visible. The brachial bridge is incomplete. The valve floor is smooth. **1a**: Ventral view. **1b**: Oblique lateral view. **1c**: Oblique anterior view. **1d**: Oblique posterior view.

Fig. 2. RBINS-RI-BRA 44, paratype. Early juvenile stage of growth with complete brachial bridge. The V-shaped structure is made of two separate spikes emerges in the middle of the valve floor. The peribrachial ridge is well-defined in the posterior part of the shell, whereas the lateral parts of the peribrachial ridge are represented only by single tubercles. **2a**: Ventral view. **2b**: Oblique lateral view. **2c**: Oblique anterior view. **2d**: Oblique posterior view.

Fig. 3. RBINS-RI-BRA 45, paratype. At this stage of growth the cardinal process is trilobed and the two spikes in the middle of the valve floor are fused at their base. The brachial bridge is entire. The peribrachial ridge is defined by a row of fused tubercles. **3a**: Ventral view. **3b**: Oblique antero-lateral view. **3c**: Oblique anterior view. **3d**: Oblique posterior view.

Fig. 4. RBINS-RI-BRA 46, paratype. In this developmental stage the major interbrachial lobes are spreading laterally and turn down anteriorly building the first stage of the "apparatus descendens". A median structure, made of two smooth ridges, is emerging on the valve floor at the base of the joined spikes. **4a**: Ventral view. **4b**: Detailed ventral view of the joined spikes. **4c**: Oblique anterior view. **4d**: Oblique antero-lateral view. **4e**: Oblique lateral view. The median ridges are clearly visible. **4f**: Oblique posterior view with the intrabrachial ridges, the slender brachial bridge and the lateral adductor muscle scars. **4g**: Detailed oblique posterior view. **4h**: Detailed oblique lateral view.

Fig. 5. RBINS-RI-BRA 47, paratype. In this growth stage the median ramus precursor emerges from the anterior part of the median ridges. A second trianglular structure appears with its base against the two central spikes and its top against the median ramus precursor (present as a knob). **5a**: Ventral view. **5b**: Detailed ventral view of the median ramus precursor. **5c**: Oblique antero-lateral view. **5d**: Oblique anterior view. **5e**: Detailed oblique anterior view. **5f**: Detailed lateral view of the major interbrachial lobe. **5g**: Oblique posterior view.

Fig. 6. RBINS-RI-BRA 48, paratype. At this stage of growth the peripheral tubercles are more or less fused and form an elevated tuberculated peribrachial ridge. Pointed processes are secreted from the central part of the interbrachial lobes reaching towards the pointed processes secreted from the spoon-like structures. The median ramus is now a wide triangle and fuse between the interbrachial lobes at the jugum. **6a**: Ventral view. **6b**: Oblique lateral view. **6c**: Oblique anterior view. **6d**: Detailed view of the pointed processes. **6e**: Oblique posterior view. **6f**: Detailed view of the jugum and the brachial bridge.

Fig. 7. RBINS-RI-BRA 49, paratype. An articulated specimen with a complete jugum. The hemispondylium is visible in the ventral valve. **7a**: Ventral view. **7b**: Detailed view of the hemispondylium. At this stage of growth the hemispondylium is attached to the ventral valve floor with a very small supporting structure (s.s.). This supporting structure is resorbed in later stages of growth. **7c**: Detailed view of the intrabrachial ridges, the major interbrachial lobes and the precursor of the median ramus.

Fig. 8. RBINS-RI-BRA 50, paratype. Detailed ventral view of a specimen with reduced residual holes in the intrabrachial ridges.

TABLE 4. Comparison of diagnostic shell characters of all valid *Ospreyella* species.

Characters	O. mutiara n. sp.	O. palauensis	O. depressa	O. maldiviana
Size of the shell	very small (W: 3.2 mm)	small (W: 4.2 mm)	large (W: 5.9 mm)	mid-size (W: 5.3 mm)
Length of pseudodeltidium	relatively long	very long	short	relatively long
Anterior commissure	slightly uniplicate to rectimarginate	rounded to slightly uniplicate	uniplicate	rounded to uniplicate
Median depression in dorsal valve	very narrow, poorly developed and strongly tuberculated in anterior part	narrow, poorly developed and slightly tuberculated in anterior part	very wide and smooth anteriorly	medium sized but poorly developed, tuberculation variable in anterior part
Ventral surface of median ramus	narrow, slightly concave, filled with secondary material	medium sized and slightly concave	wide and strongly concave	relatively wide and concave
Ramuli	strong, well defined, narrow but as wide as ramus, frilled	well defined, wide and concave	poorly defined	massive, short, well defined and concave
Major interbrachial lobes	well defined, not so massive with clearly dentate margins	massive and well defined	less defined	massive and well defined
Minor interbrachial lobes	subparallel, relatively short with asymmetrical development	subparallel to slightly divergent, medium sized	divergent and long	divergent and long
Furcation of minor interbrachial lobes	never furcating	rarely furcating or only once	furcating up to 3-4 times	furcating up to 3-4 times
Sexual dimorphic characters	marsupial notch, specialized tentacles and brood pouch in ♀	marsupial notch, specialized tentacles and brood pouch in ♀	marsupial notch, specialized tentacles and brood pouch in ♀	marsupial notch, specialized tentacles and brood pouch in ♀
Suggested reproduction mode	hermaphroditic	gonochoristic	gonochoristic	gonochoristic
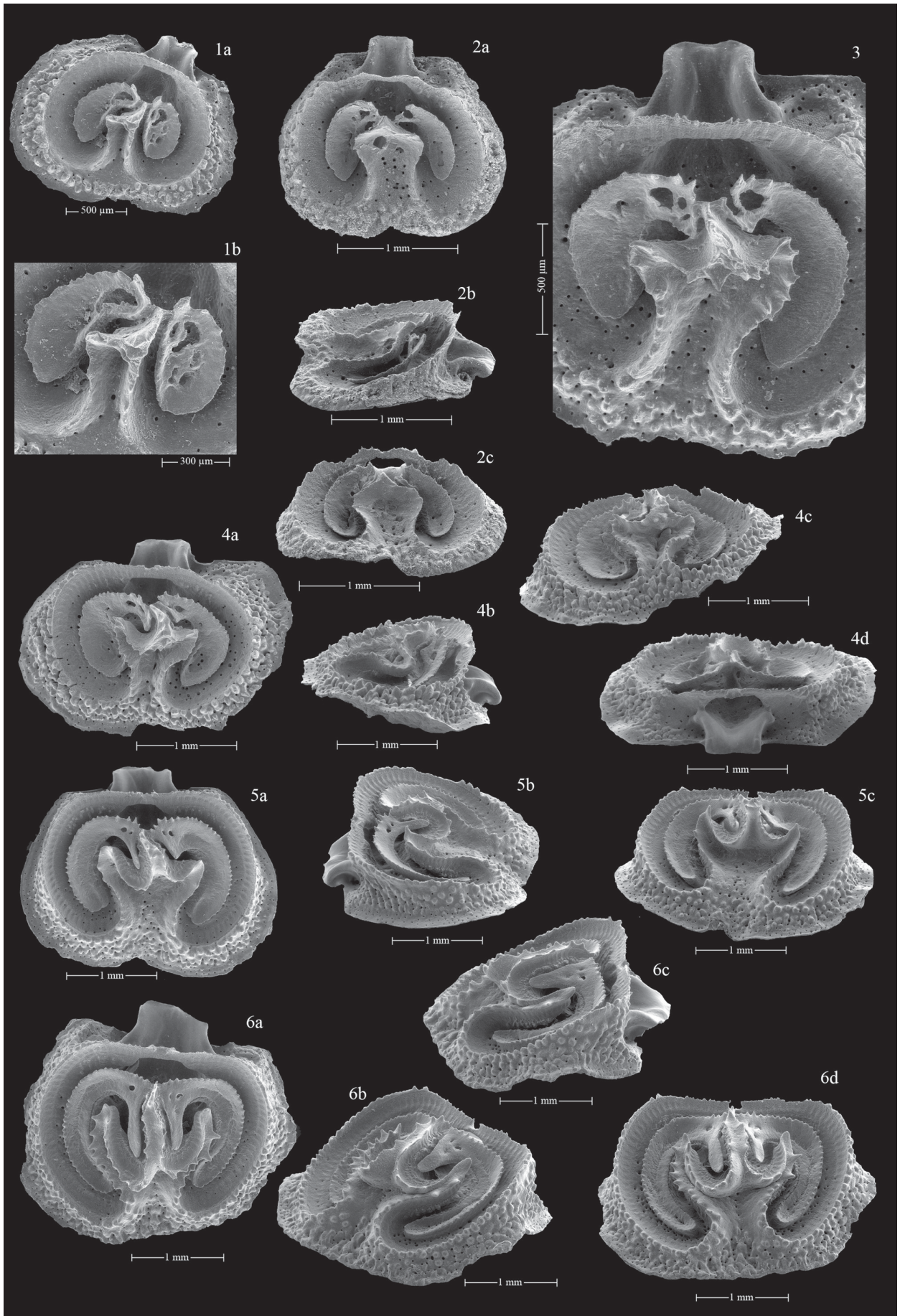
***Ospreyella* sp. (Europa Island)**
Plate 8, Figs 1a–b, 2–3, 4a–c, 5–7.

Lacazella mauritiana Dall, 1920; Zezina, 1987, p. 561.

Material investigated. The specimens illustrated in this paper (Pl. 8, Figs 1–7), deposited in the Muséum National d'Histoire Naturelle in Paris, were obtained from off Europa Island in the Mozambique Channel during the BENTHEDI – Cruise (March/April 1977) under the leadership of B. A. Thomassin (Station Marine d'Endoume, Marseille).

   Description. The shell is transversely ovate, much wider than long and the interarea is rather short (Pl. 8, Fig. 1a–b). The dorsal valve is evenly convex (Pl. 8, Fig. 1b) and exhibits a relatively wide but short median ramus, which is deeply incised and produces small interdigitations allowing the development of the minor interbrachial lobes (Pl. 8; Figs 4a, 5, 6). Two very large ramuli, much wider than the median ramus and very concave ventrally are developed. The minor interbrachial lobes are without furcations but extremely long and curved (Pl. 8, Fig. 3a). The median depression is very wide and smooth.

   Remarks. Several morphological characters observed in *Ospreyella* sp. (Europa Island) such as the structure of the median ramus and ramuli, the long and curved minor interbrachial lobes and the wide median depression suggest that this lacazelline brachiopod is in fact an *Ospreyella* species. Therefore, we place the specimens collected by the BENTHEDI - Cruise in the genus *Ospreyella*. Dall's holotype of *L. mauritiana* was collected from Mauritius which is situated 1800 km east of Europa Island, but is now lost (Logan 2005) and thus a direct comparison is not possible at the current state. New material from the type locality of *L. mauritiana* has to be collected in order to reassess the assignation of *L. mauritiana* to the genus *Lacazella* and its relationship to the specimens investigated in this study from Europa Island.

Shell ontogeny

***Minutella* cf. *minuta* (Indonesia)**

In the ventral valve the presence of the pseudodeltidium is confirmed in the earliest developmental stages and thus is a generic character of *Minutella* as already pointed out by Hoffmann and Lüter (2010, p. 155–156). The shape and the structure of the ventral valve do not change significantly throughout growth. On the contrary, the shell development of the dorsal valve follows a precise, hierarchic and complex ontogenetic development.

PLATE 7. Ontogenetic stages of *Ospreyella mutiara* **n. sp.** Size of the specimens indicated with scale bars.
Fig. 1. RBINS-RI-BRA 51, paratype. Specimen with posterior part of the median ramus bent backwards. Anteriorly a very narrow median depression appears. The major interbrachial lobes are widened and appear ovate. **1a:** Ventral view. **1b:** Detailed view.
Fig. 2. RBINS-RI-BRA 52, paratype. In this specimen the median depression is wider and more characteristic like in other representatives of the genus *Ospreyella*. **2a:** Ventral view. **2b:** Lateral view. **2c:** Oblique anterior view.
Fig. 3. RBINS-RI-BRA 33, paratype. Ventral view of the largest dorsal valve with male features. The major interbrachial lobes are elongated and the posterior portion of the median ramus is entirely pointing backwards. Two lateral ramuli are formed in correspondence with the emerging minor interbrachial lobes.
Fig. 4. RBINS-RI-BRA 53, paratype. This developmental stage is only observed in dorsal valves with female features. The marsupial notch is formed in the brachial bridge. The median ramus is a trifid structure dominated by the developing ramuli. The ventral concavity in the median ramus is filled with shell material. The major interbrachial lobes are semicircular. The asymmetrical minor interbrachial lobes are extending anterior. **4a:** Ventral view. **4b:** Lateral view. **4c:** Oblique anterior view. **4d:** Oblique posterior view with emerging marsupial notch.
Fig. 5. RBINS – RI – BRA 36, paratype. In this specimen the ramuli and the minor interbrachial lobes are extending anteriorly. The lophophore attachment muscle scars are characterised by regularly spaced small ridges. **5a:** Ventral view. **5b:** Lateral view. **5c:** Oblique anterior view.
Fig. 6. RBINS – RI – BRA 54, paratype. In this almost fully grown specimen the ramuli are slender with their central concavity closing due to successive growth. The minor interbrachial lobes are extending far anteriorly but remain without furcation. The lophophore attachment muscle scars are well-defined. **6a:** Ventral view. **6b:** Oblique antero-lateral view. **6c:** Oblique lateral view. **6d:** Oblique anterior view.
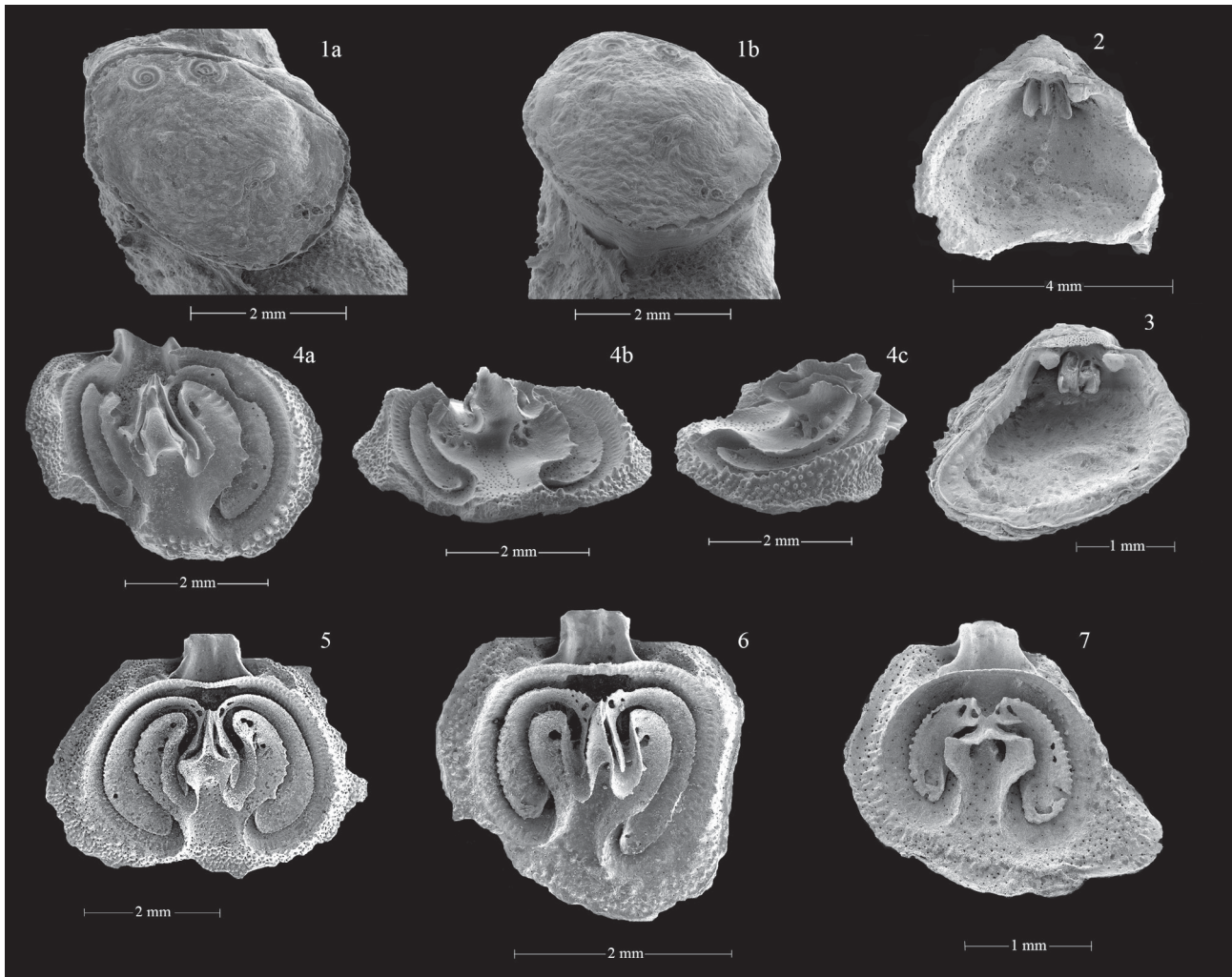
PLATE 8. *Ospreyella* sp. (Europa Island). Size of the specimens indicated with scale bars.

Fig. 1. MNHN-BRA-2312. A complete adult specimen (sex unknown) attached in living position to a dead coral. The shell of is transversely ovate, much wider than long and the interarea is rather short. **1a:** Dorsal view. **1b:** Oblique antero-lateral view.

Fig. 2. MNHN-BRA-2232. Ventral valve of an adult specimen with intact hemispondylium. (Photo A. Logan)

Fig. 3. MNHN-BRA-2232. A ventral valve of a smaller specimen seen in oblique anterior view. The anterior part of the pseudodeltidium is perforated by cavities which do not represent punctae as in *O. mutiara* **n. sp.** (Photo A. Logan)

Fig. 4. MNHN-BRA-2232. Dorsal valve of an adult specimen. The brachial bridge is broken. A long, slender minor interbrachial lobe, the jugum, the very wide and concave ramuli and the major interbrachial lobes are clearly visible. The uplifted median ramus with its narrow base is characteristic for representatives of the genus *Ospreyella*. In *Lacazella* the median ramus is entirely fused to the valve floor. **3a:** Ventral view. **3b:** Oblique anterior view. **3c:** Oblique lateral view. **3d:** Oblique posterior view.

Fig. 5. MNHN – BRA – 2232. Adult dorsal valve in ventral view with intact brachidium. The median ramus is relatively thin in this specimen but it exhibits secondary digitations. The ramuli are very wide and concave. Slightly asymetrical and relatively wide major interbrachial lobes are clearly visible. (Photo A. Logan).

Fig. 6. MNHN – BRA – 2232. Dorsal valve of another adult specimen with a still incomplete ontogenic development: the median ramus is still wide and concave, without secondary digitations. The marsupial notch is visible. (Photo A. Logan).

Fig. 7. MNHN – BRA- 2232. A juvenile dorsal valve in ventral view. The median ramu and the ramuli are poorly developed. The major interbrachial lobes are clearly visible. (Photo A. Logan).

In the earliest developmental stage found in the investigated material (Pl. 2, Fig. 2a–c) the cardinal process is short and does not extend far beyond the posterior edge of the valve. The brachial bridge is complete and already relatively broad. The peribrachial ridge is well developed on the lateral side of the valve as a row of strong tubercles. However, in the anterior part of the valve the peribrachial ridge is only a smooth ridge (Pl. 2, Fig. 2b).

The calcitic pole is missing (Pl. 2, Fig. 2c). The valve floor is free of any shell structure, smooth, and with some large punctae.

In the next ontogenetic stage the two fused sub-parallel spikes in the middle of the valve floor (Pl. 2, Fig. 3a–c) form a U-shaped structure. The cardinal process becomes more prominent but the calcitic pole is still absent (Pl. 2, Fig. 3c). In the anterior part of the valve the peribrachial ridge is now represented by a row of strong tubercles. Lateral expansions are developing on either side of the fused median spikes (Pl. 2, Fig. 4). The median septum is still absent. A pointed triangular structure appears in the middle of the dorsal side of the brachial bridge. This is the precursor of the calcitic pole.

In the next available stage (Pl. 2, Fig. 5a–c) the two central, medially fused spikes are growing backwards forming a V-shaped structure. Simultaneously, the lateral extensions build the posterior part of the intrabrachial ridges. The median septum appears in the middle of the valve floor and extends anteriorly (Pl. 2, Fig. 5b). The slender, lamellar calcitic pole is now formed and first posterior outgrowths are present (Pl. 2, Fig. 5c). A slightly more advanced stage of growth is presented in Pl. 2, Fig. 6a–b.

Later, the median septum reaches the peribrachial ridge and brachial cavity tubercles form drawing the limit of the brachial lobes (Pl. 2, Fig. 7a–b). At the next stage, more brachial cavity tubercles are progressively added and the anterior part of the median septum is bifurcate and fused as a triangular structure to the peribrachial ridge (Pl. 2, Fig. 8a–c). The ontogenetic development is finalised (in female specimens) by the completion of the brachial lobes with a brachial cover (Pl. 2, Fig. 1a–h).

Ospreyella mutiara n. sp.

In the earliest juvenile stage of growth found in the material collected from Donggala, the fundamental shell structures in the ventral valve are already developed, such as the teeth, the hinge line, the interarea and a well-defined pseudodeltidium. In the dorsal valve (Pl. 6, Fig. 1a–d) the sockets and the cardinal process are already present. The cardinal process is bilobed. Lateral adductors muscles scars are already visible (Pl. 6, Fig.1d). The brachial bridge is not complete and is formed by inwardly directed lateral growth of pointed structures which seem to be similar to the crura as described and illustrated by Logan (2008, p. 411, Figs 6.1–2). The dorsal valve floor is smooth without any spikes or spiculate construction. There is no subperipheral rim developed at this stage of growth.

Later, the crura-like shell elements form the brachial bridge by fusion (Pl. 6, Fig. 2a–d). However, at this stage the brachial bridge construction is not yet achieved (Pl. 6, Fig. 2d). A V-shaped structure consisting of two divergent spikes appears in the middle of the valve floor. The two spikes are separated from each other at their base. The lateral parts of the peripheral rim start to develop as strong tubercles. The postero-lateral subperipheral rim is well-developed and consists of two straight rims supporting the base of the cardinal process (broken in Pl. 6, Fig. 2) and the dental sockets.

In the following stage of growth, the cardinal process is trilobed (Pl. 6, Fig. 3b). The two median spikes are now fused at their base (as in Logan 2008, Fig. 6.2). The peripheral rim is completed anteriorly by several strong coalescent tubercles and a peripheral flange is perceptible. The brachial bridge is fully developed (Pl. 6, Fig. 3d).

In a later stage the divergent processes of the major interbrachial lobes which were initially growing posteriorly are bending laterally and then turn down anteriorly forming the first stages of the "apparatus descendens" (Backhaus 1959) (Pl. 6, Fig. 4a–b, 4g, 4h). This results in an M-shaped structure with its extremities slightly widened giving them a spoon-like shape. A median elongated shell structure, consisting of two faint ridges, is emerging at the anterior tip of the base of the joined spikes (Pl. 6, Fig. 4d–e).

In the following ontogenetic stage, the median ramus precursor appears as a pointed knob emerging from the anterior part of the median ridges (Pl. 6, Fig. 5a–g). This knob is the tip of a triangle emerging anteriorly (Pl. 6; Fig. 5e, 5f). These new structures are raised from the dorsal valve floor. The spoon-like structures, the precursors of the major interbrachial lobes, are widening and pointed outgrowths develop from their inner margins forming the inner margins of the major interbrachial lobes ("p" in Pl. 6, Fig. 5b).

In a further developed stage the tubercles defining the peripheral rim are more or less fused and form an elevated tuberculated rim (Pl. 6, Fig. 6a). Pointed processes arise from the central part of the intrabrachial ridges and almost reach the pointed processes secreted from the spoon-like structures of the major interbrachial lobe precursors. They are nearly fused at this stage of growth, forming subcircular holes underneath the intrabrachial

ridges (Pl. 6, Fig. 6d). In this stage the growth of the median ramus progresses and the wide triangle, elevated from the valve floor, is fused with the the intrabrachial ridges forming the jugum (Pl. 6, Fig. 6f).

In the next ontogenetic stage, the jugum is fully developed (Pl. 6, Fig. 7a–c). The lateral holes under the intrabrachial ridges are progressively reduced in size during growth. In another specimen (Pl. 6, Fig. 8) the reduced size of the holes in the intrabrachial ridges is perceptible. However, they will never be totally filled by shell material and small holes remain present even in the most adult stages observed (Pl. 7, Figs 5a, 6a). The major interbrachial lobes continue to extend anteriorly. The median ramus is widened and its apex is curving backwards. Numerous, large endopunctae are visible along the peripheral rim.

In a more advanced stage the median ramus is curved backwards and a narrow median depression is appearing anteriorly (Pl. 7, Fig. 1a–b). In another specimen (Pl. 7, Fig. 2a–c), the median depression is wider. Two lateral small, pointed outgrowths appearing at the tip of the median ramus are the ramuli precursors (Pl. 7, Fig. 1b). The two major ovate interbrachial lobes are extending anteriorly.

In the next stage in shell development (Pl. 5, Fig. 5a–e; Pl. 7, Fig. 3) the major interbrachial lobes become more elongated. The median ramus is completely pointing backwards and the two lateral ramuli are well-developed. They are concave in their central part and their external sides are ornamented with regularly spaced spines. Simultaneously, the minor interbrachial lobes are appearing. The lophophore attachment muscle scars are incipiently visible as inconspicuous small spaced vertical ridges.

The next ontogenetic stage (Pl. 7, Fig. 4a–d) is characterised by the development of the marsupial notch. The median ramus is a long trilobed structure formed by the developing ramuli. The major interbrachial lobes are now nearly semicircular. The minor interbrachial lobes are extending anteriorly and often show an asymmetrical development (rarely the length of the two minor interbrachial lobes is equal). The ventral depression of the median ramus is filled with shell material, which can also be observed for the ventral depression of the ramuli in later stages.

In the latest stages of shell development all these characters are still reinforced (Pl. 7, Fig. 5a–c). The ramuli and the minor interbrachial lobes are much longer. The lophophore attachment muscle scars made of regularly spaced small ridges are now well-developed.

In a nearly adult stage (Pl. 7, Fig. 6a–d) the ramuli are relatively long with their central depression being filled secondarily with shell secretions. The minor interbrachial lobes remain without furcation throughout their entire development.

Molecular results

The 18S data set sequence data included in this study originates from 16 thecideide brachiopod specimens. The in-group representatives are lacazelline specimens of the genus *Pajaudina*, *Lacazella* and *Ospreyella* from the Atlantic and Pacific Ocean. The four out-group representatives, such as *Thecidellina* sp. (French Polynesia), *Thecidellina williamsi*, *Thecidellina japonica* and *Minutella* sp. (Belize), belong to the subfamily Thecidellininae which is the sister group of the Lacazellinae. Removal of regions of potential alignment ambiguity in the dataset including the out-group led to the reduction of the 18S alignment from 1529 to 1502 bp (98 % retained). The maximum parsimony (MP) analyses of the 18S data set (with out-group) included 120 parsimony-informative characters and resulted in one most-parsimonious trees (tree length = 238). The 18S consensus tree with bootstrap values was calculated (not shown). The Maximum likelihood (ML) analysis of the 18S data set (with out-group) resulted in one best tree (-Ln likelihood = 3151.80958). The bootstrap values were calculated and plotted to the best tree (Text-Fig. 4). In order to confirm relationships between the lacazelline representatives, independent of the out-group, an un-rooted neighbour joining (NJ) tree was calculated (not shown).

The topologies of trees obtained with the different tree construction methods, MP, ML and NJ, did not differ, therefore only the Maximum Likelihood tree topology is described in more detail. All lacazellines representatives form one monophyletic clade which is further subdivided into two distinct clades. The monotypic genus *Pajaudina* and the Caribbean representatives of the genus *Lacazella* form one clade of solely Atlantic representatives. The *Ospreyella* species, *O. depressa* (Australia) and *O.* cf. *palauensis* (Japan) and the new species *Ospreyella mutiara*, form the second clade of Pacific lacazelline representatives only. This indicates that the taxonomic assignation of *O. mutiara* **n. sp.** to the genus *Ospreyella* and not *Lacazella* is also supported by molecular investigation.

Furthermore, there is a biogeographic separation of lacazellines into an Atlantic and Pacific clade. In-group relationships within the genus *Ospreyella* could not be resolved with this analysis, although a closer relationship between the Australian species *O. depressa* and the Indonesian species *O. mutiara* **n. sp.** is indicated.
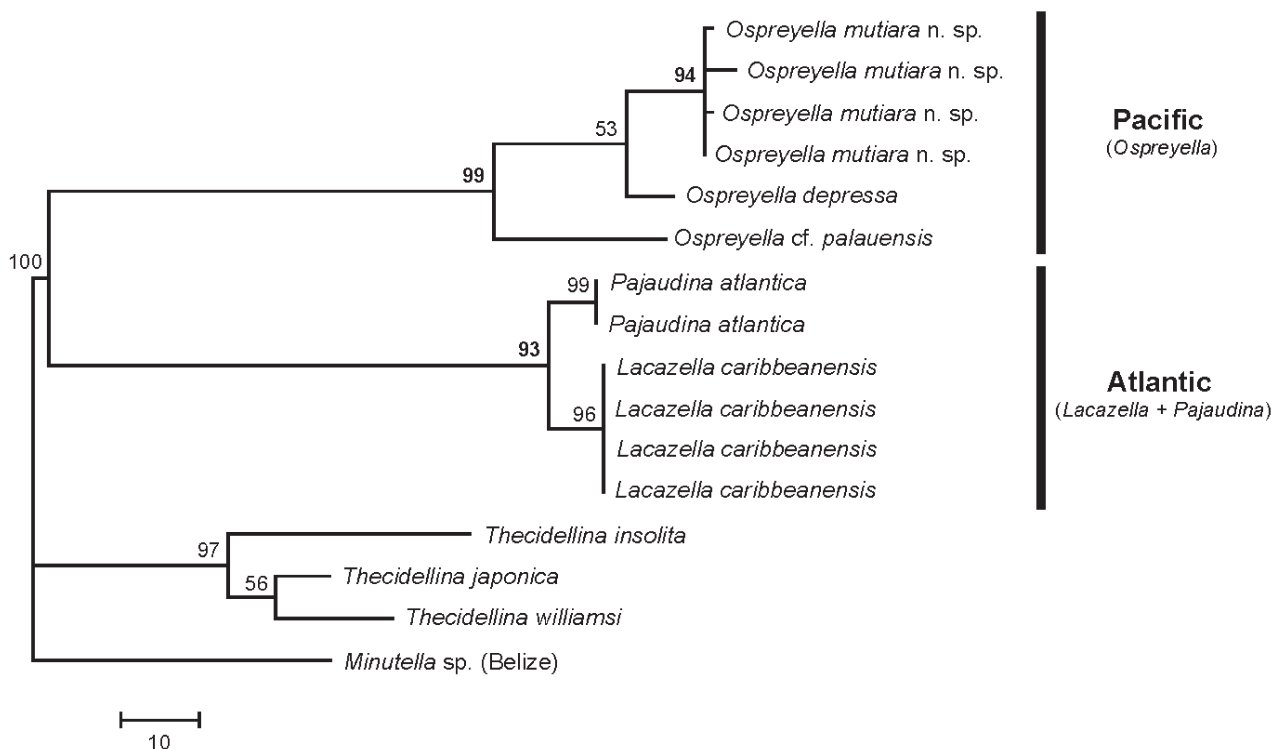
TEXT-FIGURE 4. 18S rDNA analysis, 16 sequences including four out-group representatives (*T. williamsi, T.* sp. (French Polynesia)*, T. japonica* and *M.* sp. (Belize)), Maximum Likelihood, GTR+I+G model, best tree with plotted bootstrap values, n_{reps} = 100.

Discussion

Biogeography. Despite the world-wide distribution of thecideides in the (sub)tropics this is the first documented occurrence of thecideide brachiopods at the Pacific facing side of the Indonesian archipelago. The closest known occurrence of a representative of the genus *Thecidellina*, *T. blochmanni* Dall, 1920, is Christmas Island, South of Java (Indian Ocean). Other geographically close occurrences of *Thecidellina* and the lacazelline genus *Ospreyella* are Guam and Palau in the Northeast and Lizard Island and Osprey Reef in the Southeast. The finding of thecideides in Donggala, Indonesia, thus closes an artificial gap of the distribution of thecideides in the West Pacific due to incomplete and patchy sampling. Obviously, thecideides are more widely distributed than previously thought and represent an integral component of the cryptic coral reef ecosystem.

    Habitat. This is the first documentation of thecideide brachiopods colonizing an artificial habitat. The "Mutiara", a shipwreck that is only 58 years old, offers a unique chance to study the dynamics of a brachiopod population over an ecologically short period of time without altering a natural habitat.

    The abundance of thecideide brachiopod specimens in the deeper levels of the "Mutiara", at a depth of 30 m, indicates that despite its artificial nature, this habitat seems to offer optimal conditions for settlement and establishment of a stable population. Furthermore, thecideides are the dominant brachiopod group in this part of the wreck (Simon 2010). They are known to occur in cryptic habitats, where competition with light-dependant organisms is reduced (Jackson *et al.* 1971) and competition for space becomes the most important factor (Pl. 3, Figs 3a–3b). Thus competition with other cryptic species, such as different sponges, is common (Jackson *et al.* 1971). The artificial habitat formed by the shipwreck gives us new insights into the settling abilities of thecideides. During the short period of time since this habitat was created, thecideide brachiopods were able to establish a stable population and became the most competitive brachiopod species.

Taxonomic implications including ontogeny and molecular results. In this study representatives of two thecideide genera, *Minutella* Hoffmann and Lüter, 2010 and *Ospreyella* Lüter and Wörheide, 2003, were identified. Two species are described, one recognized as *Minutella* cf. *minuta* and a new lacazelline species, *Ospreyella mutiara* **n. sp.**

The Indo-Pacific *Minutella* clade includes a number of "populations" identified as *M.* cf. *minuta* (Hoffmann *et al.* 2009; Hoffmann & Lüter 2010; this study), which are characterised by a narrow and straight median septum. Representatives of this clade are extremely uniform in most morphological characters despite their immense geographic distribution throughout the western Indian and western Pacific Oceans and also in the Red Sea (Hoffmann & Lüter 2010). The *Minutella* material collected in Donggala is also very similar to *M. minuta* s.s. from the Samper Bank and only a few morphologically-distinct characters have been observed. *M.* cf. *minuta* from Donggala possesses an even narrower median septum and the marsupial holes are more regular, subovate and relatively large with conical margins than in *M. minuta* s.s. Furthermore, the calcitic pole is thinner and produces posterior outgrowths. However, these small morphological differences are variable in the material studied and thus do not enable, for the moment, the erection of a new species. The early shell ontogeny in *M.* cf. *minuta* from Donggala corresponds very well with the shell ontogeny of other *Minutella* representatives (Hoffmann & Lüter 2010; Baker & Logan 2011). However, it differs from the Caribbean *Minutella* species *M. tristani* and *M. bruntoni* in later ontogenetic stages, when species-specific characters are formed (compare Hoffmann & Lüter 2010, Pl. 4; Baker & Logan 2011, Text-Fig. 5).

The *Ospreyella* species from Donggala has received intense scrutiny since it was first collected in 2009. In *O. mutiara* **n. sp.** a number of morphological characters, such as the narrow median ramus, the relatively narrow, poorly incised, lateral ramuli, the unfurcated minor interbrachial lobes and the absence of a median depression, initially suggested that it is a representative of the genus *Lacazella*. However, similar characters have also been found in some *Ospreyella* species. *O. palauensis* from Guam, for example, exhibits just one furcation of either of the minor interbrachial lobes (Logan 2008, p. 411). Furthermore, the supposedly juvenile *Ospreyella* specimens from Lizard Island (Hoffmann *et al.* 2009) never show any furcation of the minor interbrachial lobes and have a striking morphological similarity with *O. mutiara* **n. sp.** Apparently, the degree of furcation of the minor interbrachial lobes is a weak character for genus identification as it probably depends on the size of the shell. Therefore, several less ambiguous morphological characters that are diagnostic for the genus *Ospreyella* have been established herein. These include a free standing median ramus (initially) in the dorsal valve and the absence of a supporting septum of the hemispondylium in the ventral valve (see diagnosis). Molecular analyses now confirm that *O. mutiara* is indeed closely related to other *Ospreyella* specimens from Japan and Osprey Reef in the Pacific and clearly separated from representatives of the genus *Lacazella (*Text.-Fig. 4). Furthermore, molecular analyses support the existing lacazelline genera, which have a distinct biogeographic distribution, with *Pajaudina* and *Lacazella* in the Atlantic and Mediterranean, and *Ospreyella* in the Indopacific region. Thus, the idea that all Recent lacazelline species are representatives of one morphologically variable group with the *Lacazella* species being the most paedomorphic forms (Logan 2004) can be dismissed. Heterochrony seemingly plays a role in the establishment of these taxa (genera) but it can also be found within genera, as now illustrated for *Ospreyella*.

Reproduction modes in *Ospreyella*. We report here the first confirmation of hermaphroditism in an *Ospreyella* species, as all investigated dead shells in the sediment showed female shell characters (marsupial notch). Only in the material collected alive were small-sized specimens without a marsupial notch observed. However, because of the methods used in this study (macroscopic investigation of the gonads) no definitive statement can be made about whether small individuals exhibit only male gonads and large specimens exhibit exclusively female gonads. The case for protandry in this species must be clarified and confirmed by histological investigation of the gonads because at least one exceptional case has been documented, in a usually gonochoristic species, *Lacazella caribbeanensis*, where a fully grown individual with female shell features exhibited hermaphroditic gonads (Seidel *et al.* 2012). However, there may be some constraints that only allow larger individuals to brood larvae. A larger lophophore is advantageous as it increases the possibility of capturing more food particles and it also improves the respiratory capacity for the animal. Furthermore, the brooding of larvae requires a defined amount of space and thus a certain shell size as the brood pouch develops in the mantle cavity of the ventral valve.

Heterochrony in lacazellines. In general, shell ontogeny in lacazellines seems to be highly invariant, especially in early ontogenetic stages (Logan 2004, 2008; this study). However, shell ontogeny in *O. mutiara* **n. sp.**

is shortened in that the brachidium is not fully developed (heterochrony). There are two morphologically distinct clades in the genus *Ospreyella*, one being of relatively large shell size (max.10 mm; Lüter *et al.* 2003; Logan 2005) with a well-developed brachidium and multiple furcations of the minor interbrachial lobes and the other being of small shell size (max. 4 mm; Hoffmann *et al.* 2009; this study) with a less developed brachidum and lacking any further furcations of the minor interbrachial lobes. *O. palauensis* represents an intermediate between these forms being slightly larger (max. 7 mm; Logan 2008) and exhibiting at least one rudimentary furcation of one minor interbrachial lobe. This observation implies that shell size influences the development of the brachidium. Actually, heterochrony is known to be a common phenomenon in thecideide evolution (Jaecks & Carlson 2001). However, it remains to be seen whether the shell size can be triggered by environmental factors or is genetically fixed within a lineage. Interestingly, molecular analyses show that *O. mutiara* **n. sp.** is closely related to the type species *O. depressa* despite their differences in morphology and shell size. A dispersal event like the colonization of a new habitat could have a great effect on shell size because in order to establish a population in a short time period hermaphroditism and a small shell size enables a fast growing population despite a small initial population size. On the contrary, *O. depressa* which inhabits a very old reef body, the Osprey Reef, exhibits a large shell size, and is clearly gonochoristic. A possible explanation for this observation is that representatives of the genus *Ospreyella* are hermaphroditic and show heterochronic features when colonizing a new habitat (Seidel *et al.* 2012) but are able to switch their reproduction mode to sexual reproduction and reach a much larger shell size once a population/ species is well established. This would have important implications for phylogenetic studies as closely related species or populations could be morphologically distinct but genetically similar.

References

Backhaus, E. (1959) Monographie der cretacischen Thecideidae (Brach.). *Mitteilungen aus dem geologischen Staatinstitut Hamburg*, 28, 5–90.

Baker, P.G. (1990) The classification, origin and phylogeny of thecideidine brachiopods. *Palaeontology*, 33, 175–191.

Baker, P.G. (2006) Thecideoidea. *In*: Kaesler, R.L. (Ed.) *Treatise on Invertebrate Paleontology, Part H, Brachiopoda, Revised, 5.* Geological Society of America and University of Kansas Press, Boulder, Colorado and Lawrence, Kansas, pp. 1948–1964.

Baker, P.G. (2007) Thecideida. *In:* Selden, P.A. (Ed.). *Treatise on Invertebrate Paleontology, Part H, Brachiopoda, Revised, 6, Supplement.* Geological Society of America, Boulder, Colorado and University of Kansas Press, Lawrence, Kansas, pp. 2797–2800.

Baker, P.G. & Logan, A. (2011) Support from early juvenile Jurassic, Cretaceous and Holocene thecideoid species for a postulated common early ontogenetic development pattern in thecideoid brachiopods. *Palaeontology*, 54, 111–131.
http://dx.doi.org/10.1111/j.1475-4983.2010.01023.x

Bitner, M.A. (2010) Biodiversity of shallow-water brachiopods from New Caledonia, SW Pacific, with description of a new species. *Scientia Marina*, 74 (4), 643–657.
http://dx.doi.org/10.3989/scimar.2010.74n4643

Castresana, J. (2000) Selection of conserved blocks from multiple alignments for their use in phylogenetic analysis. *Molecular Biology and Evolution*, 17, 540–552.
http://dx.doi.org/10.1093/oxfordjournals.molbev.a026334

Cooper, G.A. (1954) Recent brachiopods. *In*: *Bikini and nearby atolls, Marshall Islands. Part 2. Oceanography (biologic). United States Geological Survey Professional Paper*, 260G, pp. 315–318.

Cooper, G.A. (1973) New Brachiopoda from the Indian Ocean. *Smithsonian Contributions to Paleobiology,* 16, 1–43.
http://dx.doi.org/10.5479/si.00810266.16.1

Cooper, G.A. (1981) Brachiopoda from Southern Indian Ocean (recent). *Smithsonian Contributions to Paleobiology*, 4, 1–93.
http://dx.doi.org/10.5479/si.00810266.43.1

Dall, W.H. (1920) Annotated list of the Recent Brachiopoda in the collection of the United States National Museum, with description of thirty-three new forms. *Proceedings of the United States National Museum*, 57 (n° 2314), 261–377.
http://dx.doi.org/10.5479/si.00963801.57-2314.261

Duméril, A.M.C. (1806). *Zoologie analytique ou méthode naturelle de classification des animaux.* Allais, Paris, XXIV + 344 pp.

Elliott, G.F. (1953) The classification of the thecidean brachiopods. *The Annals and Magazine of Natural History*, 12 (6), 693–701.

Elliott, G.F. (1958) Classification of thecidean brachiopods. *Journal of Paleontology*, 32, 373.

Gmelin, J.F. (1792) *Systema Naturae. Editio decimal tertia, aucta, reformata.* Tomus 1, Pars VI Vermes, Lipsiae (Leipzig), 888 pp.

Grant, R.E. (1983) *Argyrotheca arguta*, a new species of brachiopod from the Marshall Islands, Western Pacific. *Proceedings of the Biological Society of Washington*, 96, 178–180.

Gray, J.E. (1840) *Synopsis of the contents of the British Museum.* 42nd edit., London, 370 pp.

Hall, T.A. (1999) BioEdit: a user-friendly biological sequence alignment editor and analysis program for Windows 95/98/NT. *Nucleic Acids Symposium Series,* 41, 95–98.

Hayasaka, L. (1938) A new Neotreme genus of Brachiopod from Japan. *The Venus*, 8, 9–13.

Hedley, C. (1899) The Mollusca of Funafuti. Part II. Pelecypoda and Brachiopoda. *Memoirs of the Australian Museum,* 3, 491–510.
http://dx.doi.org/10.3853/j.0067-1967.3.1899.504

Hoffmann, J. & Lüter, C. (2009) Shell development, growth and sexual dimorphism in the Recent thecideide brachiopod *Thecidellina meyeri* sp. nov. from the lesser Antilles, Caribbean. *Journal of the Marine Biological Association of the United Kingdom*, 89 (3), 469–479.
http://dx.doi.org/10.1017/S0025315409002616

Hoffmann, J. & Lüter, C. (2010) Shell development in thecidellinine brachiopods with description of a new Recent genus. *Special Papers in Palaeontology*, 84, 137–160.

Hoffmann, J., Klann, M. & Matz, F. (2009) Recent thecideide brachiopods from the northern Great Barrier Reef, Australia (SW Pacific Ocean). *Zoosystematics and Evolution*, 85 (2), 341–349.
http://dx.doi.org/10.1002/zoos.200900010

Jaecks, G.S. & Carlson, S.J. (2001) How phylogenetic inference can shape our view of heterochrony: examples from thecideide brachiopods. *Paleobiology*, 27 (2), 205–225.
http://dx.doi.org/10.1666/0094-8373(2001)027<0205:HPICSO>2.0.CO;2

Jackson, J.B.C., Goreau, T.F. & Hartmann, W.D. (1971) Recent brachiopod-coralline sponge communities and their paleoecological significance. *Science,* 173 (3997), 623–625.
http://dx.doi.org/10.1126/science.173.3997.623

Lee, D.E. & Robinson, J.H. (2003) *Kakanuiella* (gen. nov.) and *Thecidellina*: Cenozoic and Recent thecideide brachiopods from New Zealand. *Journal of the Royal Society of New Zealand*, 33 (1), 341–361.
http://dx.doi.org/10.1080/03014223.2003.9517734

Logan, A. (1988) A new thecideid genus and species (Brachiopoda, Recent) from the southeast North Atlantic. *Journal of Palaeontology*, 62, 546–551.

Logan, A. (2004) Ecological, reproductive and ontogenetic features in *Pajaudina atlantica* Logan (Thecideidae, Brachiopoda, Recent) from the Canary Islands. *Pubblicazioni della Stazione Zoologica di Napoli: Marine Ecology*, 25, 207–215.
http://dx.doi.org/10.1111/j.1439-0485.2004.00024.x

Logan, A. (2005) A new lacazelline species (Brachiopoda, Recent) from the Maldive Islands, Indian Ocean. *Systematics and Biodiversity*, 3 (1), 97–104.
http://dx.doi.org/10.1017/S1477200004001586

Logan, A. (2008) Holocene thecideide brachiopods from the north-western Pacific Ocean: systematics, life habits and ontogeny. *Systematics and Biodiversity*, 6 (3), 405–413.
http://dx.doi.org/10.1017/S1477200008002739

Lüter, C. (2005) The first Recent species of the unusual brachiopod *Kakanuiella* (Thecideidae) from New Zealand deep waters. *Systematics and Biodiversity*, 3 (1), 105–111.
http://dx.doi.org/10.1017/S1477200004001598

Lüter, C., Hoffmann, J. & Logan, A. (2008) Cryptic speciation in the Recent thecideide brachiopod *Thecidellina* in the Atlantic and the Caribbean. *Transactions of the Royal Society of Edinburgh*, 98, 405–413.
http://dx.doi.org/10.1017/S1755691007078449

Lüter, C., Wörheide, G. & Reitner, J. (2003) A new thecideid genus and species (Brachiopoda, Recent) from submarine caves of Osprey Reef (Queensland Plateau, Coral Sea, Australia). *Journal of Natural History*, 37, 1423–1432.
http://dx.doi.org/10.1080/00222930110120971

Motchurova-Dekova, N., Saito, M. & Endo, K. (2002) The Recent rhynchonellide brachiopod *Parasphenarina cavernicola* gen. et sp. nov. from the submarine caves of Okinawa, Japan. *Paleontological Research*, 6 (3), 299–319.

Munier-Chalmas, E.P. (1880) Note sommaire sur les genres de la famille des Thecideidae. *Bulletin de la Société Géologique de France (Série 3)*, 8, 279–280.

Pajaud, D. (1970) Monographie des Thécidées. *Mémoires de la Société géologique de France, nouvelle série*, 49 (112), 1–349.

Saito, M., Motchurova-Dekova, N. & Endo, K. (2000) Recent brachiopod fauna from the submarine caves of Okinawa, Japan. *The fourth Millenium, International Brachiopod Congress, 10th – 14th July 2000.* [Abstracts]

Seidel, R., Hoffmann, J., Kaulfuß, A. & Lüter, C. (2012) Comparative histology of larval brooding in Thecideoidea (Brachiopoda). *Zoologischer Anzeiger - A Journal of Comparative Zoology*, 251, 288–296.
http://dx.doi.org/10.1016/j.jcz.2011.12.007

Simon, E. (2010) *Argyrotheca furtiva* n. sp. and *Joania arguta* (Grant, 1983) two micromorphic megathyrid brachiopods (Terebratulida, Megathyridoidea) from the Indonesian Archipelago. *Bulletin de l'Institut royal des Sciences naturelles de Belgique, Biologie*, 80, 277–295.

Tamura, K., Peterson, D., Peterson, N., Stecher, G., Nei, M. & Kumar, S. (2011) MEGA5: Molecular Evolutionary Genetics Analysis using Maximum Likelihood, Evolutionary Distance, and Maximum Parsimony Methods. *Molecular Biology and Evolution,* 28, 2731–2739.
http://dx.doi.org/10.1093/molbev/msr121

Thomson, J.A. (1915) A new genus and species of Thecidiinae. *Geological Magazine, New Series*, Decade VI, 2. 461–464.

Thompson, J.D., Higgins, D.G. & Gibson, T.J. (1994) CLUSTAL W: improving the sensitivity of progressive multiple sequence alignment through sequence weighting, position-specific gap penalties and weight matrix choice. *Nucleic Acids Research,* 22, 4673–4680.
http://dx.doi.org/10.1093/nar/22.22.4673

Williams, A., Carlson, S.J., Brunton, C.H.C., Holmer, L.E. & Popov, L. (1996) A supra-ordinal classification of the Brachiopoda. *Philosophical Transactions of the Royal Society of London*, B, 351 (4), 1171–1193.
http://dx.doi.org/10.1098/rstb.1996.0101

Winnepenninckx, B., Backeljau, T. & De Wachter, R. (1993) Extraction of high molecular weight DNA from molluscs. *Trends in Genetics,* 9 (12), 407.
http://dx.doi.org/10.1016/0168-9525(93)90102-N

Zezina, O.N. (1985) Present day brachiopods and problems of the bathyal zone of the oceans. *Instituta Okeanologii*, Akademiia Nauk SSSR, 247 pp. [In Russian]

Zezina, O.N. (1987) Brachiopods collected by BENTHEDI-Cruise in the Mozambique Channel. *Bulletin du Muséum d'Histoire naturelle*, ser. 4, 9 (A3), 551–563.

Zumwalt, G.S. (1976) *The functional morphology of the tropical brachiopod Thecidellina congregata Cooper 1954*. MS thesis (unpubl.) University of California, Davis, 135 pp.